Università di Torino

Facoltà di Medicina e Chirurgia

Anno Accademico 2010/2011

Tesi di Laurea Specialistica in Biotecnologie Mediche

# Melusin regulates ERK1/2 activation in cardiomyocytes via the Focal Adhesion Kinase and the scaffold protein IQGAP1

## Melusina regola l'attivazione di ERK1/2 nei cardiomiociti tramite la Focal Adhesion Kinase e la proteina scaffold IQGAP1

Candidato: Alessandro Bertero

Relatore: Prof. Guido Tarone

**INDEX**

**ABSTRACT**

Melusin is a muscle-specific chaperone protein that plays a key role in the protection of the heart from maladaptive hypertrophic remodeling after pressure overload, via activation of the intracellular biochemical signaling pathways of AKT and ERK1/2. Melusin forms a supramolecular complex with C-Raf, MEK1/2 and ERK1/2, and these Melusin-bound molecules are activated after pressure overload. Moreover, both the Focal Adhesion Kinase and IQGAP1, a scaffold protein involved in ERK1/2 activation, are members of the Melusin signalosome, and are required for Melusin-dependent ERK1/2 activation after pressure overload.

In the present work we first investigated the mechanisms involved in the interaction of Melusin with its binding partners IQGAP1 and FAK. We observed that Melusin CS domain directly binds two regions of IQGAP1, the IQ and RGCT moieties, and that Melusin interacts with the autoinhibitory domain of FAK.

Moreover, we analyzed the functional relevance of these interactions using cultures of mouse neonatal cardiomyocytes. We demonstrated that Melusin overexpression is sufficient to enhance basal ERK1/2 phosphorylation, and that this event triggers both increased cardiomyocyte hypertrophy and protection from apoptotic death following oxidative stress. Remarkably, we proved that FAK and IQGAP1 are both required for Melusin to fulfill all these activities.

Therefore, we concluded that Melusin is an activator of MAPK signaling in cardiomyocytes via a biochemical pathway involving FAK and IQGAP1, and that this is a crucial event that results in adaptive biological outcomes in the myocardial cells.

## INTRODUCTION

The heart is a highly dynamic organ: not only it continuously adjusts its contractile activity to meet the ever-changing needs of the organism, but it can also undergo profound structural modifications, when the altered demands are chronic. The either decreased or increased requirements for oxygen and nutrients supply from the body periphery can respectively lead to heart atrophy or hypertrophy, namely the increase or decrease in heart mass by the addition or removal of sarcomeric units (16). While the first condition affects only a minority of the population, and it is often reversible, the latter has a wide prevalence, and it can often have irreversible outcomes (25).

Heart hypertrophy is an adaptive reaction to either physiological or pathological conditions, which impose a hemodynamic overload on the cardiac walls. Indeed, as described by the Laplace's law, the increased ventricular thickness aims to decrease the stress imposed on the walls, in turn reducing their working demands (9). However, while during physiological situations, like exercise or pregnancy, the response is purely beneficial, there are detrimental consequences to the hypertrophic growth triggered by cardiovascular diseases, like aortic stenosis, hypertension, and myocardial infarction (33, 39). In fact, under these conditions, the heart is unable to maintain an adaptive remodeling over time, and eventually weakens, leading to cardiac dilation, and to the gradual development of heart failure (29).

The mechanisms underlying this transition, as well as those lying behind the different outcomes of physiological and pathological hypertrophy, are still poorly understood, but they are likely to involve an orchestrated interplay of the many cell

types that make up the cardiac tissue. However, a major role is played by cardiomyocytes, in which a complex network of intracellular signal transduction pathways finely regulates adaptive as well as maladaptive responses. In fact, while the stressed cell can thrive by adjusting its metabolism and becoming hypertrophic, under some other circumstances the burden is excessive and apoptotic or necrotic death can occur (5). At the top of the biochemical cascades involved in the regulation of these responses, there are a wide array of neuroendocrine and mechanical stimuli, whose balance deeply influences the cellular behavior (24).

Melusin is a critical mediator of these processes, as it acts as a muscle-specific sensor of mechanical stretch downstream of integrins. Using loss and gain of function genetically-modified mouse models, previous works from our laboratory demonstrated that Melusin is a key regulator of cardiomyocyte hypertrophy and apoptosis in response to mechanical overload (3, 14). In fact, during these circumstances, the ablation of Melusin leads to reduced left-ventricle hypertrophy and accelerates the evolution toward heart dilation, while, on the other hand, the forced expression of Melusin in cardiomyocytes allows the development of sustained concentric hypertrophy, and prevents the evolution towards heart failure. Moreover, there are recent evidences that Melusin overexpression in rodents can confer protection from myocardial infarction, both in the acute phase of the anoxic challenge and during the subsequent remodeling of the injured myocardium (manuscript in preparation).

From a biochemical point of view, Melusin regulates *in vivo* the phosphorylation state of two kinases, AKT and ERK1/2, that play a pivotal role in cardiomyocyte

biology (14). This, in turn, results in an increased cardiomyocyte hypertrophic growth and protection from apoptosis after chronic myocardial pressure overload.

ERK1 and ERK2 are members of the mitogen-activated protein kinases (MAPKs) family, whose activity is triggered by a variety of growth factor receptors, GPCR and adhesion molecules (46). Signalling through the ERK1/2 cascade is classically initiated at the cell membrane by the activation of the small G protein Ras, which then recruits and activates the MAP3K (MAP kinase kinase kinase) Raf. This is a serin-threonine kinase that presents three mammalian isoforms, namely Raf1 (C-Raf), A-Raf and B-Raf, that differ in their expression patterns, and that can fulfill slighlty discrepant biological roles. After activation, the MAP3K phosphorylates and activates the dual-specificity kinases MEK1 and MEK2 (MAP2Ks or MAP kinase kinases), which serve as dedicated kinases for the MAPK ERK1/2 phosphorylation and activation (32).

Active ERK1/2 can phosphorylate a wide array of more than a hundred substrates, which are located in different subcellular compartments (65). Therefore, according to the subgroup of proteins that are phosphorilated in a given cellular context, ERK1/2 can impact on many cellular processes, for example proliferation, senescence, differentiation, migration and adhesion. As a consequence, there is a strict cell specific regulation of both ERK1/2 activity and subcellular localization, which are finely tuned in order to obtain specific biological responses. Unfortunately, the details of these mechanisms are still under study (53).

In the context of cardiomyocytes, ERK1/2 is known to be activated in response to almost every stress-induced hypertrophic stimulus examined to date: G protein coupled receptors agonists (like angiotensin II, endothelin I, and epinephrine),

tyrosine kinase receptors agonists (like IGFs and FGF), cytokines, reactive oxigen species, and mechanical stretch. This suggests the straightforward hypothesis that ERK1/2 may be involved in the cardiac growth response. Indeed, data from the *in vivo* analysis of several transgenic mouse models have established ERK1/2 activation as being sufficient to trigger heart hypertrophy, even if may not be exquisitely necessary under selected circumstances (8, 22, 27, 38, 45). Moreover, these studies clearly pointed at an essential role of ERK1/2 as a protective, anti-apoptotic molecule in the heart (37, 64).

As Melusin can impact on both AKT and ERK1/2 signalling pathways, a straightforward hypothesis could be that Melusin might act via a kinase or phosphatase motif. However, this is not the case, as Melusin is characterized by domains without any known enzymatic activity, namely two N-terminal CHORD (Cysteine and Histidine Rich Domain) sites, and a CS (CHORD-containing protein and Sgt1) region in its C-terminal moiety (4). Therefore, recent efforts focused on searching the molecular partners of Melusin, in order to discover the mediators able to impact on the signal transduction pathways described above.

By using gene expression profiling, it was demonstrated that Melusin is co-regulated with heat shock proteins (55). Moreover, it was proved that Melusin can directly bind Hsp90 by means of its CHORD domains, and that Melusin has a chaperone activity per-se. Chaperones, in addition to assist the correct folding of proteins, thus preventing aggregation and degradation, play an important role in regulating signal transduction pathways, by assisting conformational changes required for protein activation (44, 62).

More recently, we obtained further clues to Melusin function by identifying novel interaction partners of Melusin (Sbroggiò M. et al, manuscript in revision for The Journal of Cell Science). We immunoprecipitated Melusin from Melusin-overexpressing mouse hearts in basal conditions or subjected to pressure overload by aortic banding (AB), and we revealed by Western blot the presence of c-Raf, MEK1/2 and ERK1/2 in the immunocomplex (Figure 1A). In agreement with the previously aforementioned results (55), we also detected the presence of Hsp90 in the complex. Interestingly, we found that the amounts of Melusin-associated MEK1/2 and Hsp90 significantly increased in response to aortic banding. The specificity of these co-precipitations was demonstrated by the fact that b-Raf, which is also expressed in the heart, was not detected in association with Melusin.

Then, to investigate if Melusin-bound MAPKs were involved in the signal transduction triggered by aortic banding, we subjected the immunoprecipitated samples to a kinase assay using recombinant ELK1 as a substrate of ERK1/2. Western blot analysis using anti-phospho ELK1 antibody demonstrated that Melusin-bound ERK1/2 were activated following aortic banding (Figure 1B). Interestingly, the specific MEK1/2 inhibitor PD89059 was able to completely abolish the AB-dependent ERK1/2 activation, indicating the involvement of MEK1/2 as an upstream kinase of ERK1/2 in this pathway (Figure 1C).

Afterwards, to clarify the mechanisms involved in the activation of Melusin-bound ERK1/2, we further analyzed Melusin co-immunoprecipitated material by using phosphotyrosine antibodies in Western blotting, and a prominent 125kDa band was clearly stained (Figure 2A). Using a panel of antibodies to signalling molecules we identified this band as Focal Adhesion Kinase (FAK) (Figure 2B). As shown, we

observed that the amount of FAK associated with Melusin was not altered by aortic banding.

FAK has a well-known pivotal role in cardiac hypertrophy and failure (19). It is an ubiquitous 125-kDa tyrosine kinase composed of an N-terminal FERM (protein 4.1, ezrin, radixin and moesin homology) domain, followed by an ~40 residue linker region, a central kinase domain, a proline-rich low-complexity region, and a C-terminal focal-adhesion targeting domain (59).

In normal conditions, FAK is maintained in an autoinhibitory conformation by an intramolecular interaction between the FERM and the catalytic domains, thus blocking the active site by inhibiting the binding of ATP (36). When FAK is activated, the tyrosine 397 within the linker region between the FERM and the catalytic domains is exposed by conformational changes and autophosphorylated, with the consequent creation of a high-affinity binding site for the Src homology 2 domains of Src family kinases. However, the mechanisms responsible for the release of the FERM moiety from the catalytic domain remain elusive. It is suspected that an activating protein, presumably docked in the FERM domain, might be responsible for disrupting the FERM/kinase interface, thus leading to FAK activation. Candidate proteins include the cytoplasmic regions of β-integrin or epidermal growth factor receptor, but cytosolic ligands may also exist (13).

Once phosphorylated, the tyrosine 397 site recruits and activates Src. This interaction leads to a cascade of tyrosine phosphorylation of multiple sites in FAK (residues Tyr576, Tyr577, and Tyr925), as well as in other signalling proteins, eventually leading to the activation of molecules like the Rho family GTPases and Ras (42). The latter signalling pathway starts when Src phosphorylates FAK at

tyrosine 925, thus creating an SH2 binding site for the GRB2 adaptor protein (42). This, in turn, triggers the canonical GRB2-SOS-Ras pathway that subsequently activates ERK1/2 (46).

FAK plays pivotal ubiquitous roles in important aspects of cell behavior such as migration, proliferation, growth, and survival. In particular, FAK is activated in cardiomyocytes by both neuroendocrine stimuli (like angiotensin II, phenilephrine and endotheline-1), and mechanical stretch (34). Studies on both isolated cardiomyocytes and transgenic models have delineated an important role for FAK in the development of heart hypertrophy (43) (15). In fact, the lack of FAK dumps the hypertrophic response after pressure overload of the myocardium, the molecular mechanism proposed to explain this phenomenon being an attenuation in ERK1/2 activation (15).

To complete the analysis of possible Melusin binding partners, we also performed mass spectrometry analysis of Coomassie blue-stained Melusin co-immunoprecipitated protein bands. Four major bands were detected with molecular weights of 190 kDa, 84 kDa, 71 kDa and 52 kDa (Figure 2C). MALDI-TOF and LC-nanospray-IT analysis identified the co-precipitated band at 190 kDa as IQGAP1 (IQ motif-containing GTPase activating protein 1), while the 84 and 52 KDa molecules were shown to be the alpha and beta subuinit of the Mitochondrial Trifunctional Protein (MTP), and finally the 71 KDa protein was identified as the chaperone Hsc70. We focused our attention on IQGAP1 for the reasons described below, and the role of the other interactors is still under investigation. As shown in figure 2D, we observed that the amount of IQGAP1 associated with Melusin did not change after aortic banding (Figure 2D).

IQGAPs (IQ motif containing GTPase activating proteins) comprise three multidomain proteins (IQGAP1, IQGAP2 and IQGAP3) sharing a similar domain structure and with considerable sequence homology (6). IQGAP proteins have different patterns of expression in mammalian tissues, IQGAP1 being the only one that has been detected in the myocardium. IQGAP1 contains different domains: calponin homology domain (CHD), poly proline protein–protein domain (WW), IQ motif (IQ), Ras GTPase-activating protein-related domain (GRD) and RasGAP_C terminus (RGCT). The calponin homology domain (CHD) is responsible for IQGAP1 binding to actin filaments; the IQ motif associates with calcium/calmodulin, b-Raf and MEK1/2; the WW domain is able to associate with ERK1/2, and the RGCT domain binds to β-catenin and E-cadherin (7). Notably, the GRD domain does not facilitate GTPase activity; rather, this domain directly interacts with and stabilizes activated Rac1 and Cdc42. Thanks to the interaction with different molecular partners, IQGAP1 regulates many cellular functions including cell proliferation, differentiation, adhesion and migration.

In particular, since it was recently reported that IQGAP1 can directly bind all the three components of the MAP kinase ERK signalling cascade (namely b-Raf, MEK1/2 and ERK1/2) (49-51), it was proposed that IQGAP1 could work as a scaffold protein for this pathway. These structural molecules are crucial regulators of the MAP kinase signalling cascade, due to their ability to bind multiple members of the pathway, and to tether them into a complex (52). In doing so, scaffold proteins boost the signal flux by increasing the proximity of the components in the complex. Moreover, scaffolds also localize the signalling molecules in particular sub-cellular compartments, thus making them responsive to selected stimuli, and influencing the

subset of substrates that can be activated downstream of ERK1/2. This, in turn, determines the final biological outcomes (31).

Regarding the role if IQGAP1 in the heart, we recently demonstrated that it has a key role in integrating hypertrophic and survival signals in cardiomyocytes, thus regulating long-term left ventricle remodeling upon pressure overload (54). We demonstrated that IQGAP1-null mice show a precise and temporally-restricted defect in the activation of ERK1/2 after pressure overload of the myocardium. This, in turn, impairs cardiomyocyte hypertrophy and increases apoptosis.

Having discovered FAK and IQGAP1 as novel interaction partners of Melusin, we investigated the possibility that they had a role in Melusin-associated ERK1/2 activation in response to pressure overload.

Firstly, as shown in figure 3A, we observed that the addition of the FAK inhibitor PF573228 totally abolished ELK1 phosphorylation in the kinase assay of the Melusin-coimmunoprecipitated ERK1/2. This result demonstrated that Melusin-associated ERK1/2 activation in response to AB depended on FAK activity. In agreement with this observation, FAK kinase assays performed on Melusin immunocomplexes demonstrated that Melusin-bound FAK was activated by AB (Figure 3B). In addition, direct immunoprecipitation of FAK from heart extracts showed an increased FAK kinase activity in response to AB (Figure 3C).

Then, we also investigated the possible role of IQGAP1, and to this purpose we took advantage of IQGAP1-null mice (35). We immunoprecipitated Melusin from Melusin-overexpressing and Melusin-overexpressing/IQGAP1-null mice hearts in sham conditions and upon aortic banding, and the immunoprecipitated samples were tested with the ERK1/2 kinase assay. As shown in figure 3D, the absence of

IQGAP1clearly reduced ERK1/2 activity, demonstrating that ERK1/2 activation in response to AB depended on the presence of IQGAP1.

All these data posed a strong background for developing a model of the Melusin-dependent biochemical pathway. During my thesis I further analyzed the relationship of Melusin with IQGAP1 and FAK, both by studying the details of the molecular interactions between these molecules, and by investigating their possible functional relationships.

I demonstrated that Melusin CS domain directly interacts with two distinct sites of IQGAP1 (the IQ and RGCT regions), nearby to the binding sites of C-Raf, MEK1/2 and ERK1/2. Moreover, I proved that Hsp90 is an IQGAP1 binding protein. These findings suggest that the chaperone activities of Melusin and Hsp90 could be responsible for the activation of the MAPK ERK1/2 pathway in the heart.

Then, I observed that Melusin binds to the FERM domain of FAK, thus posing the possibility that Melusin could regulate FAK activity by the interaction with its auto-inhibitory domain.

Finally, I showed that IQGAP1 and FAK are essential for Melusin activity in a cell culture model of neonatal mouse cardiomyocytes. In fact, both IQGAP1 and FAK are required for the Melusin-dependent upregulation of ERK1/2 phosphorylation, as well as for the consequent increase in cell hypertrophy and protection from apoptosis.

Overall, these data demonstrate that Melusin-dependent cardiomyocyte hypertrophy and survival require ERK1/2 activation by a pathway involving the chaperones Melusin and Hsp90, the kinase FAK, and the scaffold protein IQGAP1.

## MATHERIALS AND METHODS

### Recombinant proteins production.

To obtain procariotic expression vectors of MBP-fused IQGAP1 fragments, the nucleotide sequences encoding for the protein fragments indicated in figure 1A were amplified by Pfu DNA polymerase-based PCR (Promega) from a pCMVsport6 template containing full-length mouse IQGAP1 cDNA (I.M.A.G.E clone IRAVp968H1189D, RZPD). Suitable primer pairs containing restriction sites for SalI and HindIII, respectively for the forward and reverse oligonucleotides (Sigma), were used for the amplification. Afterwards, the PCR products were digested with SalI and HindIII (New England Biolabs), fractionated by agarose gel electrophoresis, and extracted with QUIAquick Gel Extraction Kit (QUIAGEN). Then, ligation was performed with a pMAL C2 vectors cut with SalI and HindIII using T4 DNA ligase (New England Biolabs), and finally E. Coli BL21 strain were transformed. Clones were screened by restriction enzymes digestion, and positive ones were further confirmed by DNA sequencing.

Vectors encoding FAK fragments were kindly provided by Brian Serrels, and their production is described in (58).

Expression vectors encoding glutathione S-transferase (GST) and maltose binding protein (MBP) fused to Melusin were prepared as previously described (55) (4), by cloning the nucleotide sequence encoding for the amino acid residues 1-320 (Melusin full-length); 1–219 (CHORD I–II) and 211–320 (CS) in pGEX and pMAL C2 vectors respectively.

To produce the recombinant proteins, their expression was induced by adding 100µM IPTG (Sigma) to transformed E. Coli during exponential growth. After 12 hours of incubation at RT in agitation, bacteria were purified by centrifugation for 30'at 3000 rpm at 4°C, and the pellets were resuspended in GST-Lysis buffer (100mM Tris-HCl pH 8, 150mM NaCl, 1% Triton X-100) or Column Buffer (20mM Tris-HCl ph 7,4, 200mM NaCl, 1mM EDTA) respectively for GST or MBP-fused fragments. Afterwards, 8 rounds of sonication were performed for 15'' at 30% amplitude using a Vibra-Cell VCX 750 (Sonics). After clearing by centrifugation for 45' at 13000 rpm at 4°C, the supernatants were aliquoted and stored at -20°C until usage.

**Pull-Down assays.**

For the pull-down experiments from heart lysates, frozen samples were first pulverized in liquid nitrogen using a mortar, and then the tissue powder was dissolved and homogenized with an Ultra-Turrax (VWR) in a lysis buffer made up of 1% Triton X-100 (Sigma) in TBS, supplemented with protease and phosphatase inhibitors (1X Protease Inhibitor Cocktail from Roche; 1mM PMSF; 1mM NaF and 1mM Na3VO4). After, three rounds of centrifugation for 20 minutes at 14000 rpm at 4°C, the protein concentration of the lysate was quantified using Bio-Rad Protein Assay, and about 1 mg of total proteins were used for each pull-down assay.

Bait proteins of MBP-fused fragments of either IQGAP1, FAK or Melusin, as well as MBP alone as control, were purified from the bacterial protein extracts described above, by using an amylose resin (GE) for 1 hour at 4°C in agitation. After five washes with lysis buffer, an aliquot of each resin, as well as known amounts of

BSA, were analyzed by SDS-Page followed by Comassie blue staining, in order to quantify the proteins. Afterwards, 5 µg of recombinant proteins were incubated with 3 mg of heart total proteins for 2 hours at 4°C in agitation. Finally, the resins were washed ten times with lysis buffer, resuspended in Laemmli buffer, and analyzed by Western blot as described below.

Pull-down experiments to evaluate the direct interaction between Melusin and IQGAP1 were performed using MBP-IQGAP1 and GST-Melusin fragments, together with MBP and GST alone as controls. Recombinant proteins were purified for 1 hour at 4°C in agitation using amylose or Gluthatione-Sepharose 4B resins (GE), respectively for MBP or GST-fused peptides. Then, resins were washed five times with an interaction buffer (50 mM Tris HCl pH 7.4; 150 mM NaCl; 1% Triton), and the GST-fused proteins were eluted from the resins for 15' at RT in agitation, using a solution of 20mM Tris and 10mM glutathione. Afterwards, the purified proteins were quantified on a Coomassie blue-stained SDS-PAGE, and 4 µmol of both resin-bound MBP-IQGAP1 fragments and eluted GST-Melusin fragments were incubated in agitation for 2 hours at 4°C in 1 ml of interaction buffer. Following incubation, resins were washed ten times with interaction buffer, resuspended in Laemmli buffer, and analyzed by Western blot.

**Co-immunoprecipitation.**

Heart samples were lysed as described above by using an immunoprecipitation buffer (50mM HEPES pH 7,2; 100mM NaCl; 0,1% Na-Deoxycholate; 0,1% Triton X-100; 2mM Na-EDTA; 1mM EGTA) supplemented with protease and phosphatase inhibitors. 5 mg of total heart proteins were incubated in agitation at 4°C with 3µg of

antibody against Hsp90 (Stressgene). After one hour, 10ul of Protein G-Sepharose (GE) was added, and following one more hour of incubation the resins were washed ten times with immunoprecipitation buffer. Finally, samples were resuspended in Laemly buffer, and analyzed by Western blot.

**Mouse neonatal cardiomyocytes cultures.**

The use of animals was in compliance with the Guide for the Care and Use of Laboratory Animals published by the US National Institutes of Health and was approved by the Animal Care and Use Committee of Turin University.

Neonatal mouse cardiomyocytes were isolated from one 1 day old mice, and a litter of 7 to 12 pups was used for each preparation. Mice strain used were: wild-type (FVB, 129sv and mixed F1 FVBx129sv), Melusin-overexpressing (FVB, described in (14)), IQGAP1-null (129sv, described in (35) and kindly provided by Wadie F. Bahou), and IQGAP1-null Melusin-Overexpressing (mixed F1 FVBx129sv).

Neonatal hearts were quickly removed from euthanized pups in sterile conditions, washed three times in cold Hank's Balanced Salt Solution (HBSS), while carefully minced to pieces of around 2 mm. Then, they were pre-digested in a solution 0.5 mg/mL Trypsin (Sigma) in HBSS, O.N. at 4°C, while shaking at 200 rpm. The following day, cells were dissociated by 4 subsequent digestion cycles for 10' at 37°C in agitation, by using a filter-sterilyzed solution of 240 U/mL Collagenase type II (Worthington) in HBSS. Cells were pooled and centrifuged at 800 rpm for 5 minutes at RT, in order to enrich the pellet of cardiomyocytes, as they are denser than non-muscolar cardiac cells (NMCC). Cells were resuspended in complete medium made up of 1:4 DMEM-M199 (Gibco), 50 mM HEPES, 5% FBS and 10%

Horse Serum (Gibco) supplemented with 1mM Penicillin and Streptomicin (Gibco). To further remove NMCC and enrich the cell population in cardiomyocytes, two rounds of pre-plating of 75' each were performed on 10 cm plastic tissue culture dishes, were NMCC adhere preferentially. After that, the supernatant was collected and alive cardiomyocytes were counted after staining with 50mM Trypan Blue (Sigma). Cells were then plated on 12-well dishes (250.000 alive cardiomyocytes) for Western Blot analysis, or on glass coverslips laid in 24-well dishes (200.000 alive cardiomyocytes) for immunofluorescence. Both dishes and coverslips had previously been coated for 2 hours at 37°C with a solution of 10mM human Fibronectin and 2% porcine gelatin (Sigma) in PBS. Cultures were mantained at 37°C with 5% CO2 in a standard incubator. The day after plating the culture medium was changed to remove unattached and dead cells, and cultures were maintained in complete medium supplemented with 1mM Cytosine Arabinoside (Sigma), in order to block the proliferation of the few contaminating NMCC.

Final cultures contained ≥90% cardiomyocytes, as determined by immunofluorescence staining for the muscle-specific marker sarcomeric α-actinin, performed as described below.

Cardiac fibroblast cultures were obtained from the pre-plating dishes aforementioned. Cells were maintained in DMEM 10% FBS and supplemented with 1mM Penicillin and Streptomicin for two days before lysis.

**Kinase inhibitors treatments.**

When indicated, neonatal mouse cardiomyocytes were treated with 50 MEK1/2 kinase inhibitor PD890959 (Calbiochem, see (17)) or 3 μM FAK kinase inhibitor

PF537228 (Tocris, see (60)). Both molecules were first dissolved in DMSO at a concentration of 50mM and 100mM respectively, and stock solutions were stored at -20°C. Final diluitions were perforemed in the complete culture medium described above. A solution of 50 µM DMSO was employed as negative control for unspecific effects of the diluent.

For cell area measurements, cells were treated from day two to four of culture, before being fixed and analyzed.

Cardiomyocytes used in experiments of apoptotic cell counts were treated 30 minutes before challenging with H202, and inhibitors were added also during the overnight recovery-time before fixation and analysis.

During the experiments for the Western blot analyses, the cells were treated at one day of culture for 30 minutes, and then they were quickly lysed following the protocol described below.

**FAK knock-down.**

FAK knock-down in neonatal mouse cardiomyocytes was performed by infecting cells with pGIPZ lentiviral particles expressing a short harpin RNA (shRNA) against FAK, as well as a GFP marker-gene (Open Biosystems, clone ID V3LMM_440799). Mock vectors carrying GFP alone were used as a control. The vectors were packaged by co-transfection of 293T cells with CMV-dR8.74 and a VSV-G envelope vector. Lentiviruses were collected after 48h from the transfection.

Cells were infected 12 hours after plating, which is at day zero of culture. After two washes, cardiomyocytes were incubated for 10 hours with pure virion-containing medium supplemented with 8µg/ml sequabrene, and afterwards fresh complete

culture medium was added. After 24 hours, viral medium was removed and replaced by complete medium. The magnitude of the infection was monitored by observing the GFP staining of transduced cells under a standard fluorescence microscope. In each experiment ≥80% cells were GFP-positive at 36-48 hours post-infection. At day four of culture, cells were either lysed for Western blot analysis of FAK expression, treated with H2O2 to induce apoptotic death, or fixed for cell area measurement.

**Measurement of apoptotic cells following oxidative stress.**

In order to induce apoptotic death of neonatal mouse cardiomyocytes, cells cultured on glass coverslips were treated with a solution of 10mM H2O2 in culture medium without serum for 10'. Then, they were washed twice with PBS to remove H2O2 and further cultured for 18h in complete medium to allow cells to either recover from the oxidative damage or undergo apoptosis. Afterwards, cells were washed twice with PBS, before being fixed for 10' at RT with a solution of 3% PFA in PBS.

TUNEL assay was performed using the "In Situ Cell Death Detection Kit TMR red" (Roche), following manufacturer's instructions. Briefly, cells were permeablized for 5' on ice with a solution of 0,1% NaCitrate 0,1% Triton X-100, washed twice with PBS, and then incubated at 37° for 1 hour with the labelling solution containing terminal deoxynucleotidyl transferase (TdT) and tetramethylrhodamine-conjugated dUTP.

After TUNEL, cells were further subjected to immunofluorescence in order to specifically stain cardiomyocytes. To this end, cells were first saturated for 1 hour at RT with a solution of 3% BSA (Sigma) in PBS, and then they were incubated with

an antibody against sarcomeric α-actinin (Sigma). After two washings in PBS, a second incubation with a secondary anti-mouse antibody was performed. For most of the experiments, the green, Alexa488-conjugated secondary antibody was used, while, for cells transduced with the shRNA against FAK and their mock controls, the blue Alexa340 fluorophore was used, as these cells express a GFP transgene. Finally, after two more washings in PBS, nuclei were counterstained with DAPI (Sigma) for 1' at RT.

Coverslips were mounted using ProLonged (Sigma) and observed at 200X under a Zeiss Apotome microscope. Then, images of random fields were collected and counts performed, by expressing the percentage of TUNEL-positive cells on the total cell number, and considering only cardiomyocites. Moreover, for cells transfected with FAK shRNA and their mock controls, only GFP-positive cells were analyzed. More than 1000 cells were counted for each point to ensure statistical reliability of the data.

**Measurement of cardiomyocyte cell area.**

Neonatal mouse cardiomyocytes were cultured on glass coverslips for the time indicated, then washed twice with PBS and fixed for 10' at RT with a solution of PFA 3% in PBS.

Cell area measurement was performed on cells stained by immunofluorescence for sarcomeric α-actinin (Sigma), as described above. The secondary antibody used was conjugated to the red fluorophore Alexa568, with the exception of lentiviral transduced cell, for which the blue Alexa340 one was used. Moreover, cardiomiocytes were stained with FITC-Phalloidin (or Texas Red-Phalloidin for GFP

expressing cells), in order to allow the precise definition of the cellular perimeter. Finally, nuclei were counterstained with DAPI.

After coverlips were mounted, cells were observed at 400X under a Zeiss Apotome microscope, images of random fields were collected, and finally analyzed using Axio Vision software (Zeiss) to calculate the cell area. At least 100 cells were measured for each experimental condition in order to guarantee statistical accurancy.

**Immunofluorescence for p-ERK localization.**

Immunofluorescence was performed on mouse neonatal cardiomyocytes as described above. A primary antibody against Phospho-T202/Y204 ERK1/2 (Cell Signaling) was used, followed by an Alexa568-conjugated secondary antibody. The actin cytoskeleton was stained with FITC-Phalloidin, and nuclei were counterstained with DAPI.

Cells were observed at 400X under a Zeiss Apotome microscope, and images of random fields were collected. Z-stack acquisitions that were parted 0,5 μm from each other were performed, and the focus plane approximately centred in the middle of the nuclei analyzed was chosen. Exposure times were hold constant thorough the analysis to ensure semi-quantitative analysis of the images.

**Western blotting**

Neonatal mouse cardiomyocytes used for Western blot analysis were cultured in 12-well plastic dishes. At the time point indicated, cells were quickly washed twice with cold PBS, then lysed with RIPA buffer (20mM Tris-HCL pH 7,5; 150mM NaCl; 1mM Na-EDTA; 1mM EGTA; 1% NP-40; 1% Na-Deoxycolate)

supplemented with protease and phosphatases inhibitors. After 10' of incubation on ice, cell debris were scraped and the lysate was cleared by centrifugation for 15' at 14000 rpm at 4°C. The supernatant was recovered, and protein concentration was determined using DC Protein Assay Kit (Bio-Rad) following manufacturer's instructions. Then, Laemly Buffer was added, and samples were boiled for 5', before being used for SDS-PAGE. 10μg of protein were loaded on 8% Acrilamide-Bisacrilamide gels.

After gel electrophoresis, proteins were transferred to nitrocellulose sheets (Whatman) by semi-dry Western bloting, and the membranes were saturated for 1 hour at 65°C with a solution of 5% BSA in TBST (0,3% Tween in TBS).

Primary antibody incubations were performed ON at 4°, and the following antibodies were used: ERK1/2; MEK1/2; AKT; Phospho-T202/Y204 ERK1/2; Phospho-S217/S221 MEK1/2; Phospo-S473 AKT; Phospho-Y397 FAK; Phospo-Y925 FAK (Cell Signalling); IQGAP1; c-Raf; b-Raf; Vimentin (Santa Cruz); Vinculin (Sigma); GST (Invitrogen); Hsp90 (Stressgene); FAK clone 2A7 (Millipore); β1D integrin (described in (2)). A monoclonal antibody against Melusin (clone C3) was recently produced in our laboratory by immunizing Melusin-null mice with recombinant GST–mouse Melusin and its reactivity was characterized in Western blot and immunoprecipitation. The epitope was mapped in the N-terminal CHORD I–II region. Antibodies were diluited in 1% BSA TBST supplemented with 0,02% Na-Azide.

Following three washings in TBST for 10' at RT, membranes were incubated for 1 hour at RT with a TBST-diluited, HRP-linked secondary antibody (Sigma).

Subsequently, after three more washes in TBST, blots were developed by using ECL Plus (Millipore) and either a Biorad ChemiDoc apparatus or standard X-ray films (Kodak). Western blot band quantifications were performed with Quantity One software (Bio-Rad).

**Statistical analyses**

The data are presented as mean ± SE. Differences between experimental groups were evaluated for statistical significance using one or two-way ANOVA with Bonferroni's correction. For all analyses, a minimum value of $P < 0.05$ was considered significant. All statistical analyses were performed using GraphPad Prism 4 (GraphPad Software version 4.0).

## RESULTS

### Melusin directly binds two distinct regions of IQGAP1 through its CS domain.

In order to gain insight into the impact of IQGAP1 on the Melusin -dependent ERK1/2 activation, we started our investigation by studying the details of the molecular interaction between Melusin and IQGAP1.

First, we produced recombinant MBP-fused fragments encompassing the N-terminal (N), middle portion (M) and C-terminal (C) of IQGAP1 (Figure 4A), and we performed pull-down experiments from Melusin-overexpressing heart lysates to test the ability of the recombinant bait proteins to bind Melusin. To our surprise, we reproducibly observed that both M and C specifically bound Melusin, despite with different affinities, the first being more potent than the latter (Figure 4A).

Then, we further detailed the regions responsible for the interaction, by using smaller recombinant fragments of the middle portion and the C-terminal of IQGAP1. As can be seen in figures 4A and 4B, only the IQ and RGCT domains specifically bound Melusin, the first proving to have a stronger affinity. Moreover, we analyzed the binding ability of truncated portions of the RGCT fragment, and we observed that only RGCT-Δ1 bound Melusin, while RGCT-Δ2 was inefficient (Figure 4A and B).

These experiments proved that IQGAP1 has two distinct binding sites for Melusin: one is located on the IQ domain (aa 717-997), and has a stronger affinity for Melusin, while the second weaker site lies close to the RGCT domain in a poorly structured region (aa 1238-1515).

On the other hand, to understand the region of Melusin involved in the binding of IQGAP1, we performed pull-down experiments from heart lysates using MBP-fused recombinant proteins of full-lenght Melusin, CHORDI-II domain and CS domain.

As shown in figure 4C, the CHORDI-II did not specifically bind IQGAP1, while the CS domain had a strong affinity, which was even higher than the one of the full-lenght Melusin, suggesting that the CHORDI-II domain might play an inibitory role in the Melusin-IQGAP1 interaction

The finding that Melusin bound IQGAP1 through a domain different from the one used for Hsp90, and the great strength of the Melusin-IQGAP1 interaction observed in immunoprecipitation experiments (Figure 2D), raised the idea that they could bind directly. To test this hypothesis, we performed in vitro pull-down experiments using Melusin and IQGAP1 recombinant fragments, respectively fused to GST and MBP.

As reported in figure 4D, full-length Melusin specifically and directly interacted with both M and RGCT-Δ1 domains of IQGAP1, with the relative affinities resembling those observed in previous experiments, M being the stronger binding partner. Moreover, we proved that the CS domain of Melusin was sufficient for the direct binding to both the regions of IQGAP1 (Figure 4E). Interestingly, the CS domain bound M and RGCT-Δ1 with comparable affinities, suggesting that the CHORD domains of Melusin could play a stronger inhibitory role in the interaction of Melusin with the C-terminal of IQGAP1 rather than with the IQ domain.

**IQGAP1 interacts with C-Raf via two distinct binding sites**

Since it was first shown that IQGAP1 interacts with B-Raf (49), all the available literature has analyzed the relationship between these two molecules, while there has

been no investigation on whether IQGAP1 could bind other Raf isoforms, namely C-Raf and A-Raf (23, 40, 41, 48). Nonetheless, it was recently reported that in NK cells stimulated via NKG2D, both B-Raf and C-Raf co-localized with Rap1 and IQGAP1, resulting in phosphorylation of the two molecules, and finally leading to ERK1/2 activation (1). Moreover, we observed that C-Raf, but not B-Raf, co-immunoprecipitated with Melusin, even if both Raf isoforms are expressed in the heart (Figure 1A).

Considering these evidences, we hypothesized that IQGAP1 could interact also with C-Raf, and we took advantage of the pull-down assay with recombinant fragments of MBP-fused IQGAP1 domains to test this possibility.

As shown in figure 5A and 5B, we noticed that C-Raf specifically interacted with IQGAP1, and, interestingly, both the middle portion and the C-terminal of IQGAP1 were capable of binding, a behavior that resembled the results obtained for Melusin. However, there were two main differences between the binding patterns of the two molecules to IQGAP1.

Firstly, although both Melusin and C-Raf interacted with the IQ domains of IQGAP1, their binding regions on the C-terminal were distinct. In fact, on the contrary of Melusin, C-Raf was not able to interact with the fragment RGCT-Δ1, while it strongly bound RGCT-Δ2 (Figure 5A and 5B). This implies that Melusin and C-Raf locate nearby, yet on different regions, of the C-terminal moiety of IQGAP1.

Secondly, the affinity of C-Raf for its two binding regions on IQGAP1 was similar, as opposite to Melusin. Moreover, it is worth noticing that C-Raf bound less strongly to the IQ domains alone than the complete M fragment (Figure 5B), suggesting that the WW domain of IQGAP1 can co-operate with the IQ domain to

further the interaction of C-Raf. However, a similar behavior was not observed for Melusin.

One last finding of the experiment shown in figure 5B is that we could detect no binding of B-Raf to any of the IQGAP1 fragments tested, despite B-Raf being expressed in the heart. This suggests that in the cellular context of cardiomyocytes IQGAP1 selectively interacts with C-Raf rather than B-Raf, although the reasons underlying this phenomenon are unclear, and they are still a subject of investigation.

**Melusin is not required for C-Raf, MEK1/2 and ERK1/2 binding to IQGAP1.**

Having discovered that Melusin can directly interact with IQGAP1, we asked how they could co-operate to maximize ERK1/2 activation. As Melusin does not have any kinase domain, its only known activity being as a chaperone protein, a straightforward hypothesis was that Melusin could alter the binding of some of the components of the MAPK cascade to IQGAP1. Indeed, it was previously shown that in epithelial cells there is an increase in MEK1 binding to IQGAP1 after EGF stimulation, resulting in increased ERK1/2 phosphorylation (51). This suggested that a similar mechanism could be involved in Melusin-dependent ERK1/2 activation in cardiomyocytes.

However, as shown in figure 5C, pull-down experiments with GST-fused IQGAP1 fragments proved that the absence of Melusin did not alter the binding of C-Raf, MEK1/2 and ERK to IQGAP1. Moreover, aortic banding imposition did not alter the binding of MAPK signaling components to IQGAP1 either in presence or absence of Melusin (data not shown).

It is worth noticing that we observed that both MEK1/2 and ERK1/2 bound to the middle portion of IQGAP1 as previously reported (50, 51), while no binding occurred with the C-terminal moiety, further supporting the specificity of C-Raf and Melusin interaction to the latter region of IQGAP1 (Figure 5C).

**IQGAP1 is an Hsp90-binding protein.**

As we proved that Melusin does not alter quantitatively the binding of C-Raf, MEK1/2 and ERK1/2 to IQGAP1, one possibility was that Melusin could impact on the activity of those molecules via its chaperone activity per se, as well as by the recruitment of Hsp90. As a matter of fact, both C-Raf and MEK1/2 are well-recognized Hsp90 client proteins (20), but there was no report on whether IQGAP1 could bind to Hsp90.

Indeed, we observed that IQGAP1 specifically co-immunoprecipitated with Hsp90 from heart lysates (Figure 5D). Moreover, the binding of Hsp90 to IQGAP1 was unaltered by the removal of Melusin, implying that IQGAP1 can be linked to a chaperone activity also independently of Melusin.

This result suggested that Melusin and Hsp90 could contribute to IQGAP1-dependend MAPK activation by their chaperone activity on some of the protein involved in the signaling cascade.

**Melusin binds to the FERM domain of FAK**.

After having investigated the details of the molecular interactions between Melusin and the MAPK signaling molecules with IQGAP1, we turned our attention to the Focal Adhesion Kinase.

We performed pull-down experiments from Melusin overexpressing mouse hearts using MBP-fused FAK fragments encompassing the first and the second half of the molecule (N and C, figure 6A) in order to detect Melusin binding. We observed that only the N moiety of FAK interacted specifically with Melusin (Figure 6B). Since this region comprises both the FERM and kinase domain of FAK, we further tested whether the FERM domain alone could still bind to Melusin, by using a GST-fusion protein of this portion. As shown in Figure 6C, this was the case (Figure 6C), so we concluded that the Melusin binding site on FAK lies on the FERM domain. As this region is crucial in the regulation of FAK activity (18), this finding rose the interesting possibility that Melusin binding could directly influence the kinase activity of FAK either by simple binding or by means of Melusin chaperone activity. This possibility, however, is still under study.

As regards to Melusin, despite many efforts, we unfortunately could not set up an efficient pull-down protocol using MBP-fused Melusin fragments to reveal FAK binding. This might be due to an unknown defect in the bacterial-produced recombinant proteins that affected the interaction with FAK.

**Establishment of a model for the *in vitro* study of Melusin function**.

As we had collected plenty of information about Melusin molecular partners and their interactions, and we had some hypothesis about how they might co-operate to trigger ERK1/2 activation, we then wanted to unravel the biological relevance of this network of molecules. To this aim, we decided to establish an in vitro cell culture model of neonatal mouse cardiomyocytes (NMC), and we took advantage of the Melusin-overexpressing mice to compare their properties to wild-type counterparts.

We adopted a culture protocol which successfully allowed the reproducible purification of ≥90% viable and beating cardiomyocytes. These cells were positive for the cardiac-specific markers sarcomeric α-actinin and β1D Integrin, while they were negative for the mesenchimal lineage marker Vimentin (Figure 7A and 7B). Moreover, as shown in figure 7C, NMC already expressed high levels of the Melusin transgene driven by the αMHC promoter, so they were a suitable model to study the effect of Melusin overexpression.

**Melusin-overexpressing neonatal cardiomyocytes show hyperactivation of the MAPK signaling pathway.**

As a first step, we tested whether Melusin overexpression in NMC was able per se to increase the activation of signaling pathways that we had already observed to be hyper activated in vivo in the adult heart of Melusin-overexpressing mice (14).

Out of many different conditions tested (see discussion), we observed that Melusin-overexpressing NMC cultured under steady-state conditions in a medium complete with serum showed a reproducible increase in MEK1/2 and ERK1/2 phosphorylation compared with wild-type (Figure 8A and 8B). However, we could detect no up-regulation of Akt phosphorylation, in contrast with the results previously obtained in vivo. The reasons for this behavior are still unclear. Finally, the phosphorylation status of FAK was unaltered, in agreement with the results obtained with *in vivo* experiments, where we observed that the overexpression of Melusin did not alter the phosphorylation of FAK after aortic banding (Mauro Sbroggiò, data not shown).

We then analyzed the subcellular distribution of activated ERK1/2 in Melusin-overexpressing and wild-type NMC by immunofluorescence staining of phosphorylated ERK1/2. As reported in figure 8C, wild-type NMC showed a perinuclear enrichment of phospo-ERK1/2, with nuclear staining being minimal. On the contrary, a strong nuclear localization of activated ERK1/2 was constantly observed in Melusin-overexpressing cells.

**Melusin-dependent ERK1/2 hyperactivation requires both FAK and IQGAP1.**

Having obtained a reliable model of Melusin-dependent ERK1/2 hyperactivation, we then tested the role of FAK and IQGAP1 in this phenomenon.

As far as FAK is concerned, we took advantage of PF573228, a recently-identified, highly-selective pharmacological inhibitor of its kinase activity (60). Treatment of NMC with this molecule for 30 minutes almost completely abolished FAK phosphorylation on tyrosine 397, an autophosphorylated residue that indicates the level of FAK activity (Figure 9A). In turn, FAK inhibition resulted in a down-regulation of ERK1/2 phosphorylation in both wild-type and Melusin-overexpressing NMC, the final levels not being statistically different. This implied that under these experimental conditions, FAK played an important role in ERK1/2 activation, and that Melusin-dependent boosting of this signaling pathway required normal FAK kinase activity.

Then, to investigate the role of IQGAP1, we decided to use a genetic approach, by exploiting an IQGAP1 knock-out mice model previously characterized (35). We crossed these mice with our Melusin-overexpressing ones, in order to obtain a double transgenic IQGAP1-null and Melusin-overexpressing line. While the absence of

IQGAP1 *per se* did not impair ERK1/2 phosphorylation in NMC cultured in the absence of specific stimuli, the lack of IQGAP1 clearly abolished the Melusin-dependent hyperactivation of ERK1/2 in the same conditions (Figure 9B).

**Melusin-overexpression triggers cardiomyocyte hypertrophy, and confers protection from apoptosis**.

To further investigate the functional relationship between Melusin and its binding partners FAK and IQGAP1 in the activation of ERK1/2 signalling pathway, we wanted to switch from the biochemical perspective to the analysis of the cellular outcomes. As ERK1/2 activation has been widely reported to positively regulate cardiomyocyte hypertrophy and protection from apoptosis (30), we analyzed whether this was the case in our model.

First, we analyzed by immunofluorescence the cell area of wild-type and Melusin-overexpressing NMC at different time points after isolation. As can be seen in figure 10B, over the first four days of culture both wild-type and Melusin-overexpressing cells showed a remarkable increase in cell area, with transgenic ones being significantly bigger at day four compared with their wild-type counterparts (Figure 10A).

Then, we challenged NMC with H2O2 to induce oxidative-stress, and we analyzed the extent of cellular apoptosis using a TUNEL assay. Again, we compared wild-type and Melusin-overexpressing NMC at different time points of culture. While there were no significant differences for cells treated at day two, it was clear that at day four the transgenic cardiomyocytes were significantly protected from the induction of apoptosis (Figure 10C and 10D).

**IQGAP1, FAK and MEK are required for Melusin-induced cardiomyocyte hypertrophy.**

Having understood the conditions in which we could observe the cellular outcomes of Melusin overexpression in NMC, we tested whether FAK and IQGAP1, as well as the MAPK pathway, were required for Melusin to fulfill these activities.

To start with, in figure 11A we report the results of pharmacological experiments aimed to study the hypertrophic response of NMC, in which wild-type and Melusin-overexpressing cells were treated with a FAK or a MEK1/2 inhibitor, respectively PF573228 and PD89059. We chose to start treating cells at day two of culture, when, as previously shown, we did not observe any difference between wild-type and transgenic ones. Then, we measured the cell area after 48 hours of treatment with the inhibitors, namely at day four, a time point in which Melusin-overexpression proved to induce increased hypertrophy.

Neither of these interventions impaired the hypertrophic growth of wild-type NMC cultured with complete medium over the treatment period, while the addition of either of the molecules completely abolished the gain in terms of cell area that were triggered by the overexpression of Melusin (Figure 11A).

The blunting effect of the MEK1/2 inhibitor was somehow expected, as it had already been demonstrated that it could block the hypertrophic growth of neonatal rat cardiomyocytes infected with a lentivirus carrying a Melusin transgene (14). However, the striking similarity of the effects obtained when treating with the FAK inhibitor was a new finding. When this is considered together with the biochemical

data previously shown, it strongly suggests that MEK1/2 and FAK lie on the same molecular pathway triggered by Melusin to induce hypertrophic growth.

Since pharmacological experiments with kinase inhibitors can potentially suffer from non-specific effects on off-targets enzymes, we adopted a complementary approach to confirm the reliability of our results, by knocking-down the expression of FAK with a lentivirus carrying a specific shRNA. We infected cells at day zero of culture, in order to allow some time the efficient expression of the shRNA, which was monitored through the reporter gene GFP. We observed that at 36-48 hours post-infection the intensity of the GFP fluorescence reached a peak, so we assumed that this protocol would allow mimicking the experimental conditions of the pharmacological treatments, where the kinase activity of FAK was blocked at a comparable time point. Lentiviral infection was highly efficient with ≥80% GFP positive cells, and we could successfully reduce the expression levels of FAK by 80% in NMC (Figure 11B).

As expected, knocking-down the expression of FAK blunted the hypertrophic advantage of Melusin-overexpressing cardiomyocytes analyzed at day four of culture (Figure 11C). On the other side, the shRNA against FAK did not impair the cell area of wild-type NMC, nor did the mock infection significantly impact on the hypertrophy of both transgenic and wild-type cells.

Afterwards, we turned our attention on IQGAP1, by analyzing the cell area of NMC obtained from the IQGAP1-null, Melusin-overexpressing line at day four of culture. As reported in figure 11D, the double transgenic cardiomyocytes were indistinguishable from wild-type ones and significantly smaller than the single

transgenic, Melusin-overexpressing cells. Moreover, the deletion of IQGAP1 alone did not alter the normal hypertrophic growth of NMC in culture.

Therefore, these experiments demonstrated that both IQGAP1 and FAK are required for the proper pro-hypertrophic activity of Melusin in NMC, and that this is likely to occur via MEK1/2-ERK1/2 activation.

**IQGAP1 and FAK are required for Melusin-induced cardiomyocyte hypertrophy.**

At this point, we asked whether the anti-apoptotic effect of Melusin relied on the same signaling pathway that we identified being able to trigger cardiomyocyte hypertrophy. To this end, we started by treating day four wild-type and Melusin-overexpressing cardiomyocytes with FAK and MEK inhibitors 30 minutes before challenging them with H2O2, and we analyzed the apoptotic response to understand the effects of the pharmacological interventions.

Remarkably, we observed that both inhibitors completely impaired the protective effects due to the overexpression of Melusin in NMC, while they had only a minimal effect on the induction of apoptosis in wild-type counterparts, figures not being statistically different from DMSO-treaded controls (Figure 12A).

Moreover, the same experiments were conducted on NMC in which the expression of FAK had been knocked-down by the shRNA according to the protocol described earlier, confirming that FAK was required for Melusin to reduce the extent of apoptotic death after oxidative stress (Figure 12B). Interestingly, under our experimental conditions, the reduction of FAK expression from day two to four of

culture of NMC had an exquisite effect only on Melusin-overexpressing cells, and not on wild-type counterparts.

Finally, we repeated the experiments using IQGAP1-null and Melusin-overexpressing cardiomyocytes, and, similarly, we observed that the lack of IQGAP1 completely blunted the reduction in cardiomyocyte apoptosis after H2O2 treatment owing to Melusin overexpression (Figure 12C). It is important to notice that IQGAP1-null NMC were slightly more prone to apoptotic death after oxidative challenging (Figure 12D).

All things considered, we thus proved that the Melusin-dependent protection from apoptosis in cardiomyocytes requires both IQGAP1 and FAK, and that their activities *bona fide* impact on the activation of MEK1/2-ERK1/2 signaling pathway.

## DISCUSSION

Our previous findings demonstrated a key role of Melusin in triggering a compensatory hypertrophic response after long standing pressure overload, thus preventing left ventricle dilation and heart failure. We showed that Melusin is a chaperone molecule regulated by mechanical stress (55), which is capable of activating AKT and ERK signalling after pressure overload of the myocardium.

More recently, we observed that Melusin is able to interact with all the three components of the MAPK signalling pathway (C-Raf, MEK1/2 and ERK1/2), and it is part of a molecular complex that also includes the Focal Adhesion Kinase (FAK), the scaffold protein IQGAP1, and the chaperone protein Hsp90 (Sbroggiò et al, manuscript in revision for The Journal of Cell Science). Analysis of this protein complex in hearts subjected to pressure overload indicated that Melusin-bound ERK1/2 is activated in response to AB, and that its activation is dependent on MEK1/2, FAK and IQGAP1. In fact, specific inhibition of the kinases MEK1/2 and FAK abolished ERK1/2 activation in response to AB, and the same happened when IQGAP1 was removed by a genetical approach. Also, we noticed that recruitment of MEK1/2 and Hsp90 to the Melusin-IQGAP1-FAK complex was significantly enhanced by AB, suggesting a potential mechanism by which ERK1/2 activation could be obtained.

In fact, since Melusin binds Hsp90 and possesses a chaperone activity per se, we previously proposed a role for Melusin as a co-chaperone in the Hsp90 machinery (55). Hsp90 is able to bind and protect a wide range of substrates or ‘‘client proteins’’ from degradation, and has a key role in signal transduction due to its

ability to maintain proteins in a three-dimensional conformation that favours their activation (44).

The MAPK pathway involves a cascade of three kinases (C-Raf, MEK1/2 and ERK1/2), that sequentially activate each other by phosphorylation. A key role in regulating such cascades is played by scaffold proteins that enhance signal efficiency by assembling the molecules involved in signal transduction in close proximity. IQGAP1 is a widely expressed multidomain protein regulating different aspects of cell physiology and capable of binding to distinct signalling molecules (7). Emerging evidence indicate that IQGAP1 acts as a scaffold for the MAPK cascade by binding B-Raf, MEK1/2 and ERK1/2, and regulating their activation in response to selected stimuli (52). Scaffold proteins bind multiple members of a signaling pathway in order to tether them into complexes thus enhancing signaling efficiency.

The scaffold role for the MAPK signaling pathway of IQGAP1 was first discovered in models of epithelial cell lines (51), but subsequent works showed that this activity is fulfilled in many different cellular contexts, like fibroblasts, endothelial cells, NK cells and neurons (1, 41, 49, 56). Moreover, results from our laboratory recently showed that also cardiomyocytes subjected to pressure overload depend on IQGAP1 for a precise and temporally restricted wave of ERK1/2 activation. Moreover, this event is required for the heart in order to maintain an adaptive hypertrophic remodeling over time, as the lack of IQGAP1 causes decreased hypertrophy and increased apoptosis of cardiomyocytes, thus leading to early functional decline of the myocardium (54).

These findings raise the possibility that the MAPK scaffolding role of IQGAP1 is ubiquitous, however, it is likely that tissue specific factors influence IQGAP1

activity to direct specific cellular responses. Melusin, being a muscle-specific protein involved in the activation of ERK1/2 after pressure-overload of the myocardium, and being a binding partner of IQGAP1, is a good candidate to play such a role in the cardiomyocyte context.

FAK is an ubiquitously expressed non-receptor tyrosine kinase acting as a primary integrin effector at focal adhesion sites (42). Several reports in the literature indicated FAK as a crucial transducer for ERK1/2 activation downstream of integrins and growth factor receptors (21, 42, 61). A mechanism involved in ERK1/2 activation by FAK consists in the recruitment of the adaptor protein Grb-2 on FAK C-terminal region, thus leading to the activation of the small GTPase Ras via the guanosine exchange factor SOS. However, FAK-mediated and Ras-independent ERK1/2 activation has been reported in a number of experimental systems (12, 26, 59). Since Ras and Grb-2 have not been detected in the Melusin supramolecular complex (Sbroggiò Mauro, data not shown), we hypothesized that FAK controls ERK1/2 activation in a Ras-independent way.

To sum up, according to the aforementioned data, we postulated the hypothesis that Melusin, by interacting with FAK, IQGAP1, C-Raf, MEK1/2, and ERK1/2, regulates the MAPK pathway via Hsp90 recruitment and its own chaperone activity. In line with this hypothesis is the fact that FAK, C-Raf and MEK1/2 are known Hsp90 client proteins (55, 57). We hypothesized that both the IQGAP1 scaffold and the chaperone proteins Melusin and Hsp90 are needed to fully activate the ERK1/2 pathway in response to pressure overload in the heart. In fact, it is known that ERK1/2 activation requires chaperones for stimulus-dependent conformational

changes and scaffold-mediated assembly of the three MAP kinases signalling complex (11).

Starting from these background hypotheses, here we showed the molecular details about how Melusin can bind to IQGAP1 and FAK, and we exploited this information to propose some speculations about how these interactions can result in increased ERK1/2 phosphorylation in the heart. Moreover, we proved that both IQGAP1 and FAK are required for Melusin-dependent cardiomyocyte hypertrophy and protection from apoptosis, which are triggered by ERK1/2 activation.

First of all, we showed that Melusin interacts with two regions of IQGAP1. The first binding site, namely the IQ motif, is the region that was reported to be bound by B-Raf and MEK1/2 (49, 51), and here we demonstrated that also C-Raf interacts with IQGAP1 through this domain. Moreover, the WW domain, that was demonstrated to be the ERK1/2 binding site on IQGAP1 (50), is adjacent to the IQ, lying closely to its N terminal. This implies that the IQGAP1-bound Melusin is settled in proximity to all the three members of the MAPK ERK1/2 signalling cascade. This localizaton may be foundamental in order to allow the Melusin-dependent potentiation of ERK1/2 activation by means of Melusin chaperone activity as well as with other, still unknown, mechanisms. Moreover, we also showed that Hsp90 is an IQGAP1 binding protein, thus implying that there are at least two molecules capable of a chaperone activity that interact with IQGAP1, and that can potentially regulate the activation of IQGAP1-bound signalling molecules. It is worth noticing that Melusin is not required for the binding of MAPK signalling molecules to IQGAP1, but this was someway expected, as these interactions were first discovered in non-myocardial cells, where Melusin is not expressed (51). Therefore, we propose that Melusin acts

as a cardiac specific chaperone that potentiates the ubiqiutous IQGAP1-dependent ERK1/2 activation pathway in response to stress.

As C-Raf, MEK1/2, ERK1/2, and Melusin share binding sites lying on the same region of IQGAP1, it is likely that steric interactions impede that a single IQGAP1 molecule simultaneously binds all these proteins. Moreover, it was previously shown that all the members of the MAPK pathway directly interact with IQGAP1 (49, 50, 51). We showed here that also the binding of Melusin to IQGAP1 is direct, thus ruling out the possibility that the interaction may be mediated through any of the other molecules present in the complex. Therefore, in order for IQGAP1 to fulfill its scaffold role, it is likely that IQGAP1 oligomeric structures exist, in which a single scaffold binds one or few signalling proteins, in order to bring in close proximity all the molecules required for the succesful activation of the pathway. A similar mechanism was demonstrated in yeast cells, where dimerization of the scaffold protein Ste5 is required for the activation of ERK1/2 (63). Indeed, it is known that IQGAP1 can dimerize and even tri-tetramerize through its central region, and that this interaction is functionally relevant (47).

The second direct binding site of Melusin on IQGAP1 lies on its C-terminus, specifically in the region that follows the GRD domain and encompasses the RGCT region. Interestingly, we proved that also C-Raf interacts within a close, yet distinct, region. However, we could not observe any binding of neither MEK1/2 nor ERK1/2 in the same region. Therefore, only some of the molecules involved in the MAPK signalling patwhay are present on the C-terminus of IQGAP1. The significance of this finding is, however, still unknown. A possible interpretation of the data is that this region may work as a further docking site for some molecules, Melusin and C-

Raf, which might be required at high concentration in the IQGAP1 signalosome in order to obtain a complete activtion of ERK1/2.

As regards to the IQGAP1 binding site on Melusin, we demonstrated that the CS domain is sufficient for the interaction. We previously showed that Melusin directly interacts with Hsp90 via its CHORD region (55). Therefore, at least on a theorical basis, Melusin could simultaneously bind to both IQGAP1 and Hsp90, by means of its two different domains. This property may be important for the localization of Hsp90 nearby to IQGAP1, in order to direct the Hsp90 chaperone activity on the IQGAP1-bound signalling molecules. We showed that Hsp90 can bind IQGAP1 even in the absence of Melusin, suggesting that Melusin is not absolutely required for the interaction. Nonetheless, our finding that Hsp90 association to Melusin increases after pressure overload implies that Melusin can increase Hsp90 recruitment to the IQGAP1 signalosome after stimulation.

Another important finding is that the CS domain binds to IQGAP1 more effectively than full-lenght Melusin, suggesting that the CHORD domain plays an inhibitory role on this interaction. A similar behaviour was previously reported in regards with the binding of Melusin with the cytoplasimc tail of the integrin β1D (4), and we have evidences that also other interactors of Melusin may bind stronger to the CS domain alone than to full-lenght Melusin (unpublished data). It is known that, in plant cells, two proteins homologues to the CHORD and CS domains, respectively Rar1 and Sgt1, directly bind to each other (66). Therefore, it is forseeable that also Melusin CHORD region interacts with the CS moiety, and we have some indications that this is indeed true (unpublished data). At in all, these findings suggest the interaction of Melusin with most of its binding partners may be regulated by an

intramolecular interaction between the CHORD domains and the CS region. Whether this latter property is dynamically regulated *in vivo* to adjust Melusin activation according to different stimuli is not currently known.

As far as FAK is concerned, we showed that Melusin can bind this molecule on its FERM domain. This region is known to mediate an autoinhibitory role on FAK kinase activity, by binding the kinase domain, thus preventing access of ATP to the catalytic site (36). There are few known molecules that can relieve this inhibition by competing with the kinase region for the binding to the FERM domain. An early report described such a role for the cytoplasmic tail of the integrin β1 (13), and another mechanisms was proposed recently, involving the binding of phosphatidylinositol 4,5-bisphosphate with a basic patch of the FERM domain (10). It is likely that there are still other ligands capable of triggering the activation of FAK, and our data suggest that Melusin could be one of these molecules. This notion, however, requires further experiments to be demonstrated.

To sum up, even if a complete description of every interaction between the molecules involved in Melusin signal transduction will require further studies, we demonstrated here how Melusin interacts with its binding partners IQGAP1 and FAK. These data support the notion that a macromolecular complex involving Melusin, FAK, IQGAP1, Hsp90 and the MAPK signalling molecules might exist, and suggest some hypothesis to understand how the cooperation of the different activities of chaperone, kinase and scaffold proteins could co-operate in order to trigger ERK1/2 activation in the heart after stress.

In the second part of this work, we wanted to investigate the functional relevance of the Melusin-associated signalosome in cardiomyocytes. To this aim, we choosed

to employ a model of neonatal mouse cardiomyocyte cultures, as this offered many advantages compared to *in vivo* studies.

In fact, we wanted to be able to easily manipulate the experimental conditions by using pharmacological or genetic approaches, which are difficult and time consuming *in vivo*. Moreover, as we wanted to study the role of ubiquitous molecules such as FAK and IQGAP1, *in vivo* studies would require complex approaches of tissue-specific inhibition in order to avoid suffering from unspecific effects.

Another point was that the vast majority of data about Melusin function had been previously obtained *in vivo*, with few experiments proving that Melusin could work in a cell autonomous fashion. In fact, the heart is a complex organ made up of many different cell types, with cardiomyocytes being numerically less than half of the total population, and there are complex interactions between these different entities both by means of secreted factors and cell surface molecules. Moreover, the blood flow in the heart constantly alters the composition of the cardiomyocytes microenvironment by the provision of nutrients and hormones.

Finally, by using neonatal mouse cardiomyocytes we could exploit the Melusin overexpressing transgenic line that we previously generated as a powerful tool to study Melusin function.

First, we tried to reproduce the biochemical data obtained in vivo, namely that Melusin overexpression triggers increased ERK1/2 and AKT activation both under basal conditions and after aortic banding (14). To this end, we tried different culture conditions, in order to find the best circumstances that evidenced Melusin activity. We observed that neither under serum starvation nor after acute stimulation with serum there were reproducible evidences of increased ERK1/2 phosphorylation in

Melusin-overexpressing cardiomyocytes (data not shown). However, when cells were cultured under steady state conditions with complete medium, there was a strong upregulation of ERK1/2 activation triggered by Melusin overexpression. It is worth noticing that this culture protocol is likely to better mimic the in vivo situation, in which the blood flow provides a continuous supply of nutrients and growth factors, with little fluctuations in their concentrations. An acute stimulation with serum, in fact, is hardly comparable with any *in vivo* situation. The lack of evidence of a role for Melusin in ERK1/2 activation after serum stimulation may result from the interference of the many growth factors that are known to activate ERK1/2, therefore possibly hiding a Melusin-dependent effect. On the other hand, the finding that the lack of any stimulation by growth factors in the culture medium was equally unable to evidence any Melusin-dependent ERK1/2 activation, raised the interesting possibility that signals others than mechanical stretch could be necessary to activate Melusin. This notion differs from what we previously proposed about Melusin being an exquisite mechanical sensor through its interaction with the integrin β1D (3), but it is nonetheless possible that the signals arising from growth factors may simply contribute to outside-in signaling to integrins, thus contributing to their activation (28). The specific molecules required for this process are, however, still not known.

An important observation is that under all the culture conditions tested, we could not observe any Melusin-dependent hyperactivation of AKT. The reasons of this discrepancy with the data previously obtained in vivo are unclear. A possible explanation might be that we did not mimic the signals arising from mechanical stretch in our cultures. Another possibility is that the activation of AKT downstream of Melusin may be dependent on the interaction of cardiomyocytes with the cardiac

extracellular matrix, as well as with other non-myocardial cells. These processes, in fact, were not reproduced *in vitro*.

When we analyzed the localization of phosphorylated ERK1/2, we observed that there was a strong enrichment of active ERK1/2 in the nucleus of Melusin-overexpressing cardiomyocytes, while wild-type counterparts showed little nuclear localization, but a heavy perinuclear one. It is well-recognized that the subcellular localization of ERK1/2 has a profound impact on the biological outcomes following its activation (46). As ERK1/2 was reported to play a crucial role both in maladaptive and adaptive remodeling (8, 27), it was postulated that these differences might lie in a divergent set of ERK1/2 substrates activation, which in turn depends on the subcellular localization of active ERK1/2. Indeed, a recent report showed that nuclear translocation of ERK1/2, which depends on a phosphorylation event on the threonine 188, is required for the development of maladaptive cardiomyocyte hypertrophy (38). As we observed a massive Melusin-dependent nuclear translocation of phosphorylated ERK1/2, yet this phenomenon is likely beneficial, as proven by the data previously obtained *in vivo*, we believe that ERK1/2 activity is more complexly regulated than how it was described. In fact, the nuclear localization may not be exquisitely linked to a maladaptive remodeling, but the influence of other still unknown factors may play an important role in determining the consequences of ERK1/2 activation. For example, scaffold molecules are well-recognized molecular tools that regulate the set of substrates available to phosphorylation by ERK1/2 (11). In this context, we propose that IQGAP1 might be responsible for the selective activation of an adaptive hypertrophic program. This notion is supported by our recent finding that the lack of IQGAP1 predisposes the heart to early functional

decline after pressure overload via reduced ERK1/2 activity in a temporally defined manner (54).

To understand the role of IQGAP1 and FAK on Melusin-dependent ERK1/2 activation in mouse neonatal cardiomyocytes, we inhibited these molecules by means of genetic or pharmacological approaches. These experiments revealed that both IQGAP1 and FAK are functionally required for Melusin-dependent increase in ERK1/2 phosphorylation. It is worth noticing that, while the lack of IQGAP1 had no effect on ERK1/2 activity under steady state culture conditions, the inhibition of FAK considerably reduced the level of ERK1/2 phosphorylation in the same context. The first finding is consistent with the data that we previously obtained *in vivo*, as the analysis of IQGAP1-null hearts showed no defect neither in basal nor after short-term pressure overload (54). In fact, the dramatic defect in ERK1/2 activation was evident only after four days of aortic banding. Nonetheless, we observed an identical behavior in hearts from Melusin-null mice (unpublished data). At in all, this suggest that during resting conditions, Melusin has little or no influence on ERK1/2 activity, while it is strictly required when there is a persistent stress that is challenging the cardiomyocyte. According to this idea, the hyperactivation of ERK1/2 consequent to Melusin overexpression may be the result of a basal activation of this signaling pathway, which occurs even in the absence of any specific stimulation.

However, the decrease of ERK1/2 phosphorylation after the pharmacological inhibition of FAK implies that this molecule is also involved in the basal ERK1/2 activation, perhaps via signaling pathways independent from Melusin. Indeed, it is known that FAK is a crucial mediator of neuroendocrine-induced ERK1/2 activation

(34). Nonetheless, our experiments clearly demonstrated that FAK activity is totally required for the overexpressed Melusin to increase ERK1/2.

To explore the biological consequence of Melusin-dependent ERK1/2 activation, we analyzed the extent of hypertrophy and the sensitivity to oxidative stress-induced apoptosis of Melusin-overexpressing cardiomyocytes. Indeed, we proved that these cells are more hypertrophic and more resistant to apoptosis than wild-type ones, confirming previous results obtained *in vivo* (14). Interestingly, we observed that both these effects were evident only after four days of culture. This is not likely to be due to a weak expression of Melusin during the first days of culture, as transgenic Melusin is already highly-expressed after the isolation of neonatal cardiomyocytes. Moreover, the biochemical analyses presented here were performed at day one of culture. Therefore, the time required for the display of Melusin-dependent phenotypes might be a simple reflection of a time-consuming process involving the activation of transcription factors, and eventually the alteration of the genetic expression. We also have preliminary evidences that the release of one or more soluble factors is involved in the hypertrophic growth of Melusin-overexpressing cardiomyocytes (unpublished data). Indeed, this process would require longer time to be completed than a simpler cell-autonomous signaling cascade.

Importantly, we demonstrated that MEK, FAK and IQGAP1 are all required for both the increased hypertrophy and the decreased sensitivity to apoptosis that is consequent to Melusin overexpression. Interestingly, the inhibition of all these molecules had no effect on the hypertrophic growth that occurs in wild-type cardiomyocytes over the four days of culture. As no specific stimulus, yet only serum, was applied over this period, this kind of growth is likely comparable to the

physiological hypertrophy that occurs in cardiomyocytes during the normal development on an organism. In line with this interpretation, it is the fact that our data are consistent with results obtained *in vivo* in transgenic mouse lines that abolished the expression of ERK1/2, FAK or IQGAP1 (15, 54, 45). In fact, in all these models cardiomyocytes undergo normal hypertrophic growth during development, implying that other signaling pathway might bypass the need for ERK1/2 activation during this process (24). However, as we showed here, ERK1/2 activation is mandatory to mediate the increased hypertrophic growth triggered by Melusin overexpression.

In regards to apoptosis susceptibility, the lack of any effect after MEK inhibition in wild-type cardiomyocytes treated with H2O2 is partially unexpected. In fact, it was reported that ERK1/2 is a protective, anti-apoptotic molecule in vivo in the stresses heart (45). This finding might be due to the particular experimental conditions that we employed, in which the acute oxidative damage induced a massive apoptotic death of almost half of the cells. That situation was hardly comparable to the *in vivo* setting, in which the damage is gradual and the apoptotic death occurs over a long period of time. Therefore, these experimental conditions might have been unsuitable to show an effect of ERK1/2 on the protection from apoptosis in wild-type cells. However, it is clear from our data that ERK1/2 activation via FAK and IQGAP1 is required for the overexpressed Melusin to play its protective role against apoptotic death

On the other hand, it is important to mention that we observed how the lack of IQGAP1 increased the apoptotic death of cardiomyocytes under the same experimental conditions. This may be explained as IQGAP1 has pleiotropic roles

apart from ERK1/2 activation, as for example it is required for the phosphorylation of AKT, a well-known anti-apoptotic molecule (54). This finding complicates the interpretation of the data that we obtained in the double transgenic Melusin-overexpressing and IQGAP1-null cells, as the lack of Melusin-induced protection from apoptosis might have been partially dependent on Melusin-independent mechanism involving other functions of IQGAP1. However, our experiments as a whole strongly suggest that IQGAP1, FAK and Melusin lie on the same molecular pathway, thus enabling us to conclude that IQGAP1, like FAK and ERK1/2, is required as well for Melusin-dependent protection from apoptosis.

A last point worth being discussed is whether the increased resistance to oxidative damage of Melusin-overexpressing cardiomyocytes is a consequence of their hypertrophic phenotype or not. As the genetic experiments that used double transgenic Melusin-overexpressing and IQGAP1-null cells, or that exploited the shRNA against FAK, induced a lack of Melusin-dependent hypertrophic growth before the oxidative challenging, they do not rule out the possibility that the former phenotype is the primary cause of the decreased sensitivity to the stress. However, the pharmacological experiments were performed by adding the inhibitors only thirty minutes before oxidative challenging, and therefore they acted on fully-hypertrophic Melusin-overexpressing cardiomyocytes. As the results obtained with the two approaches were identical, we conclude that the hypertrophic growth and the resistance to apoptosis are two independent phenotypes that are triggered by Melusin overexpression.

In conclusion, in this work we proved that the stress-responsive protein Melusin is able to increase ERK1/2 activation in a cell-autonomous fashion in mouse neonatal

cardiomyocytes. This phenomenon is responsible for an increased hypertrophic growth, as well as a reduced susceptibility to apoptotic death induced by oxidative stress, and relies on the activity of IQGAP1, FAK and MEK1/2. These molecules form a signalosome in the heart together with the other members of the MAPK signaling pathway C-Raf and ERK1/2, and the chaperone proteins Hsp90 and Melusin. The combined activity of all these molecules is the key to the efficient activation of the final mediator ERK1/2, which in turn triggers the adaptive biological outcomes in myocardial cells.

**FIGURES**

## Figure 1

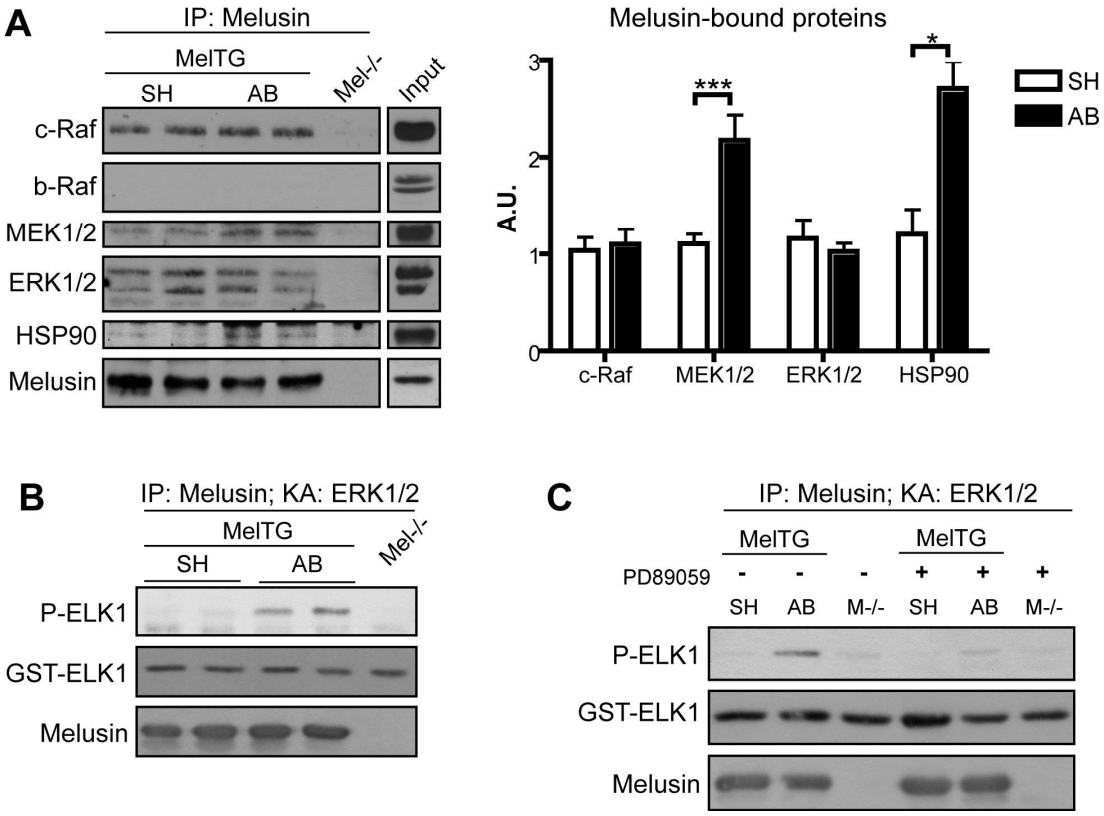

## Figure 2

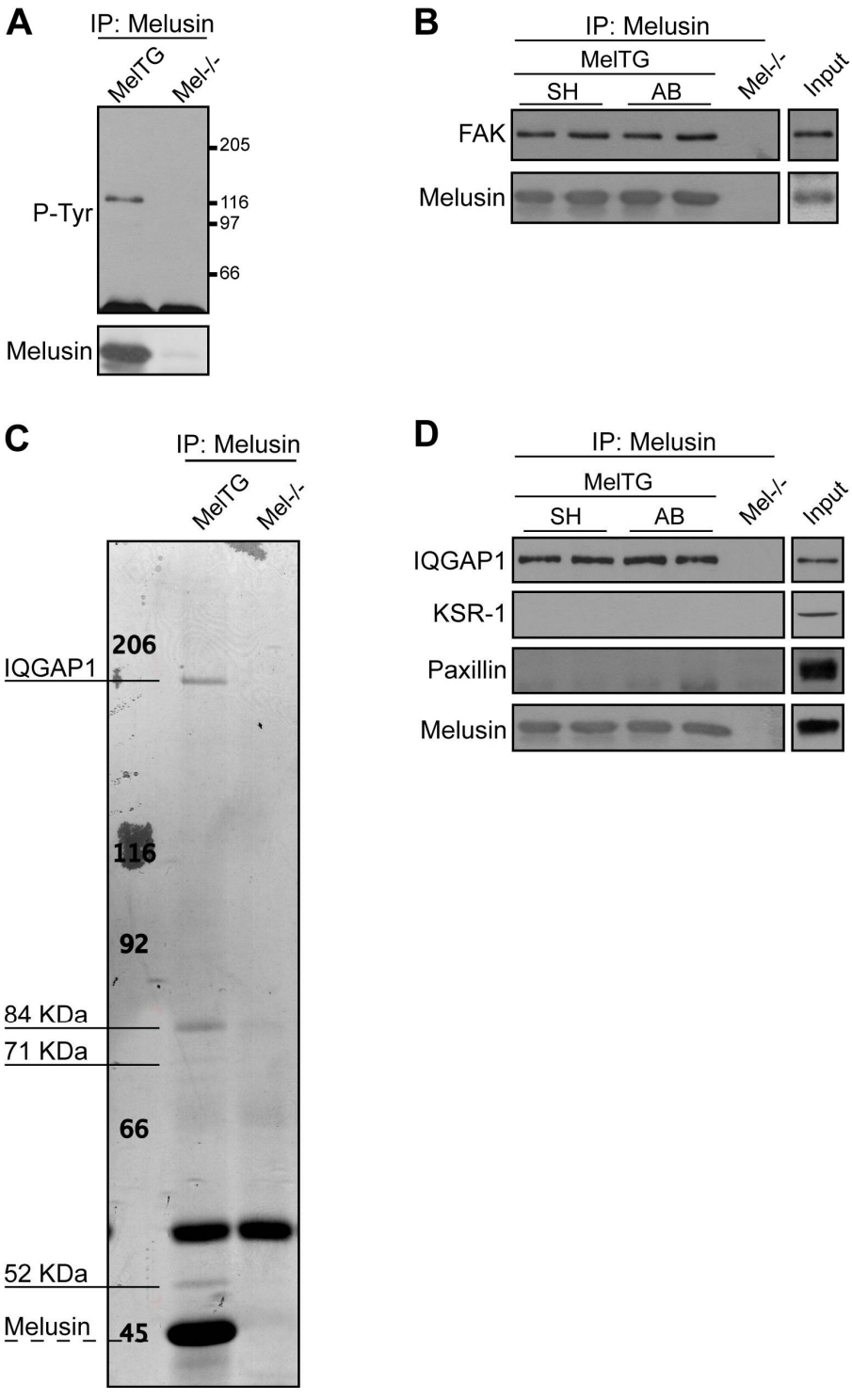
A
IP: Melusin
MelTG
Mel-/-
205
116
97
66
P-Tyr
Melusin
B
IP: Melusin
MelTG
SH
AB
Mel-/-
Input
FAK
Melusin
C
IP: Melusin
MelTG
Mel-/-
IQGAP1
206
116
92
84 KDa
71 KDa
66
52 KDa
Melusin
45
D
IP: Melusin
MelTG
SH
AB
Mel-/-
Input
IQGAP1
KSR-1
Paxillin
Melusin

## Figure 3

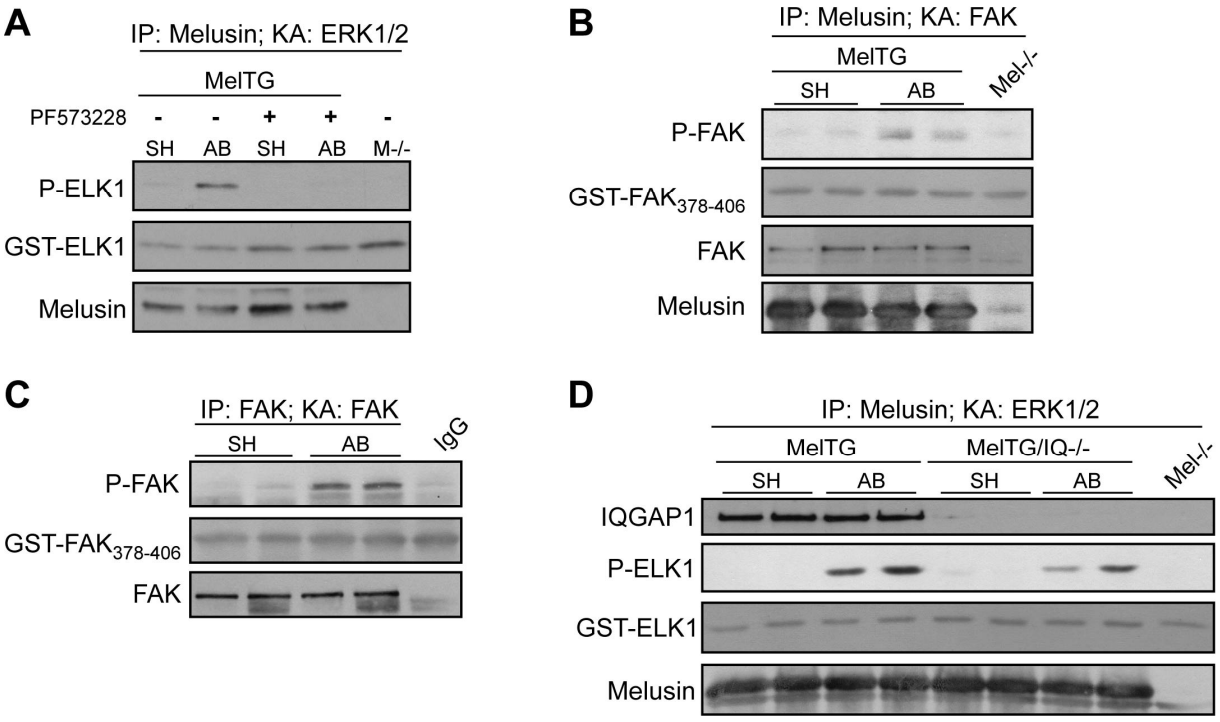
A
IP: Melusin; KA: ERK1/2
MelTG
PF573228 - - + + -
SH AB SH AB M-/-
P-ELK1
GST-ELK1
Melusin
B
IP: Melusin; KA: FAK
MelTG
SH AB
Mel-/-
P-FAK
GST-FAK378-406
FAK
Melusin
C
IP: FAK; KA: FAK
SH AB
IgG
P-FAK
GST-FAK378-406
FAK
D
IP: Melusin; KA: ERK1/2
MelTG
MelTG/IQ-/-
SH AB SH AB
Mel-/-
IQGAP1
P-ELK1
GST-ELK1
Melusin

# Figure 4

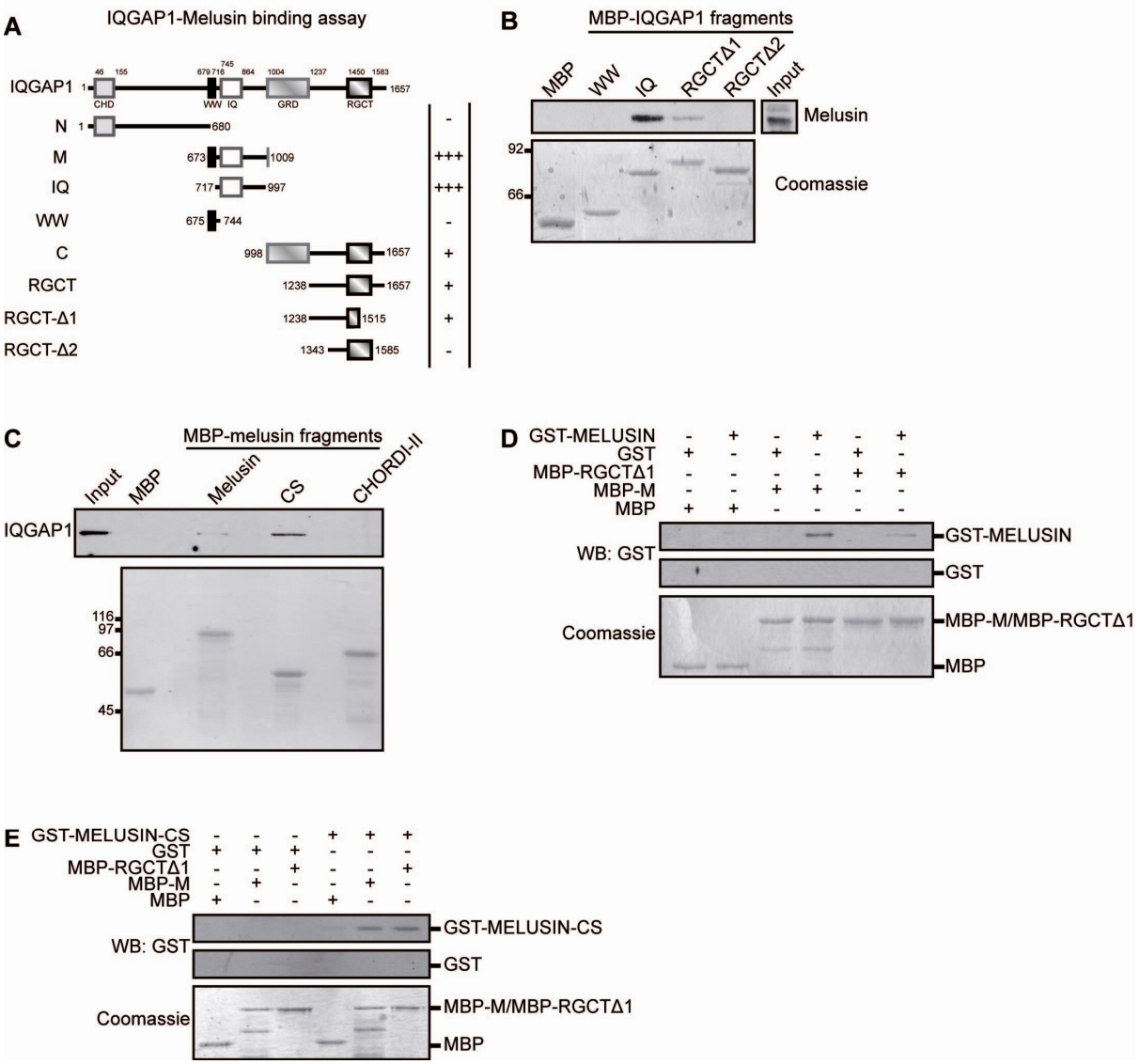
A
IQGAP1-Melusin binding assay
IQGAP1
N
M
IQ
WW
C
RGCT
RGCT-Δ1
RGCT-Δ2
CHD
WW IQ
GRD
RGCT
B
MBP-IQGAP1 fragments
MBP
WW
IQ
RGCTΔ1
RGCTΔ2
Input
Melusin
Coomassie
92
66
C
MBP-melusin fragments
Input
MBP
Melusin
CS
CHORDI-II
IQGAP1
116
97
66
45
D
GST-MELUSIN
GST
MBP-RGCTΔ1
MBP-M
MBP
WB: GST
Coomassie
GST-MELUSIN
GST
MBP-M/MBP-RGCTΔ1
MBP
E
GST-MELUSIN-CS
GST
MBP-RGCTΔ1
MBP-M
MBP
WB: GST
Coomassie
GST-MELUSIN-CS
GST
MBP-M/MBP-RGCTΔ1
MBP

## Figure 5

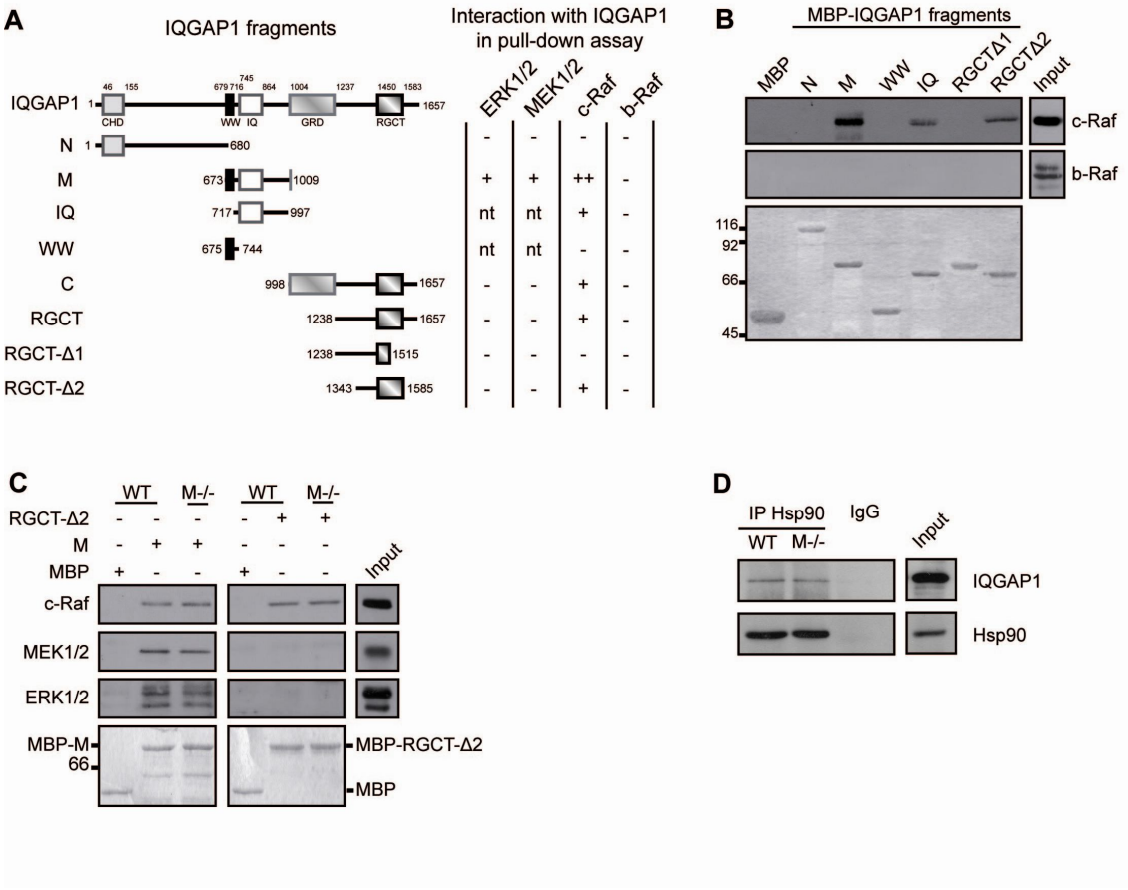
A
IQGAP1 fragments
Interaction with IQGAP1 in pull-down assay
ERK1/2
MEK1/2
c-Raf
b-Raf
IQGAP1
N
M
IQ
WW
C
RGCT
RGCT-Δ1
RGCT-Δ2
CHD
WW IQ
GRD
RGCT
B
MBP-IQGAP1 fragments
MBP
N
M
WW
IQ
RGCTΔ1
RGCTΔ2
Input
c-Raf
b-Raf
116
92
66
45
C
WT
M-/-
WT
M-/-
RGCT-Δ2
M
MBP
Input
c-Raf
MEK1/2
ERK1/2
MBP-M
66
MBP-RGCT-Δ2
MBP
D
IP Hsp90
IgG
WT
M-/-
Input
IQGAP1
Hsp90

## Figure 6

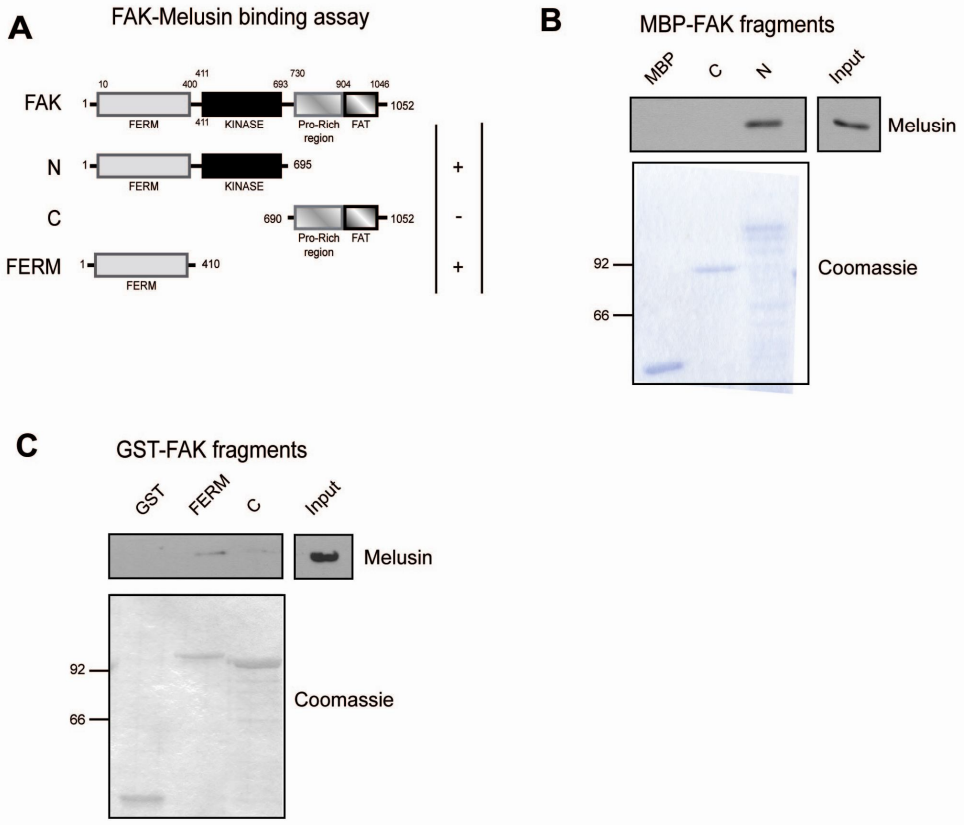
A
FAK-Melusin binding assay
FAK
N
C
FERM
FERM
KINASE
Pro-Rich region
FAT
+
-
+
B
MBP-FAK fragments
MBP
C
N
Input
Melusin
Coomassie
92
66
C
GST-FAK fragments
GST
FERM
C
Input
Melusin
Coomassie
92
66

**Figure 7**

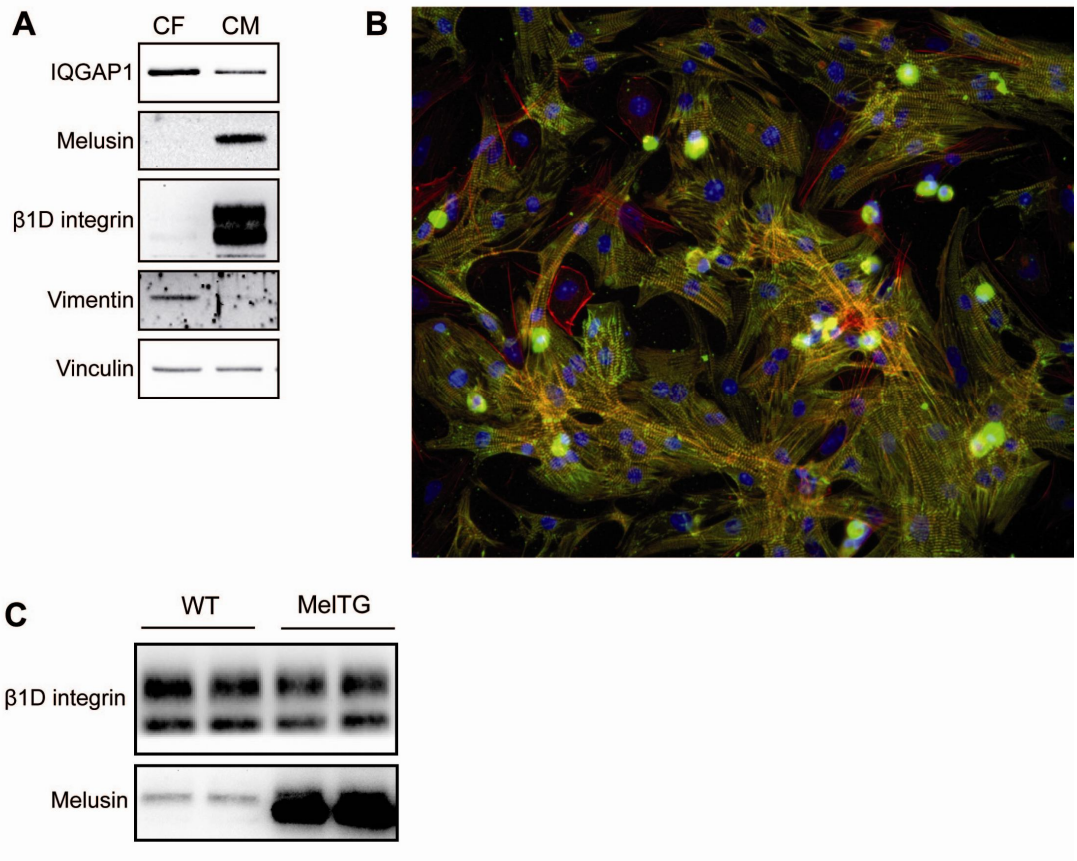
A
CF
CM
IQGAP1
Melusin
β1D integrin
Vimentin
Vinculin
B
C
WT
MelTG
β1D integrin
Melusin

## Figure 8

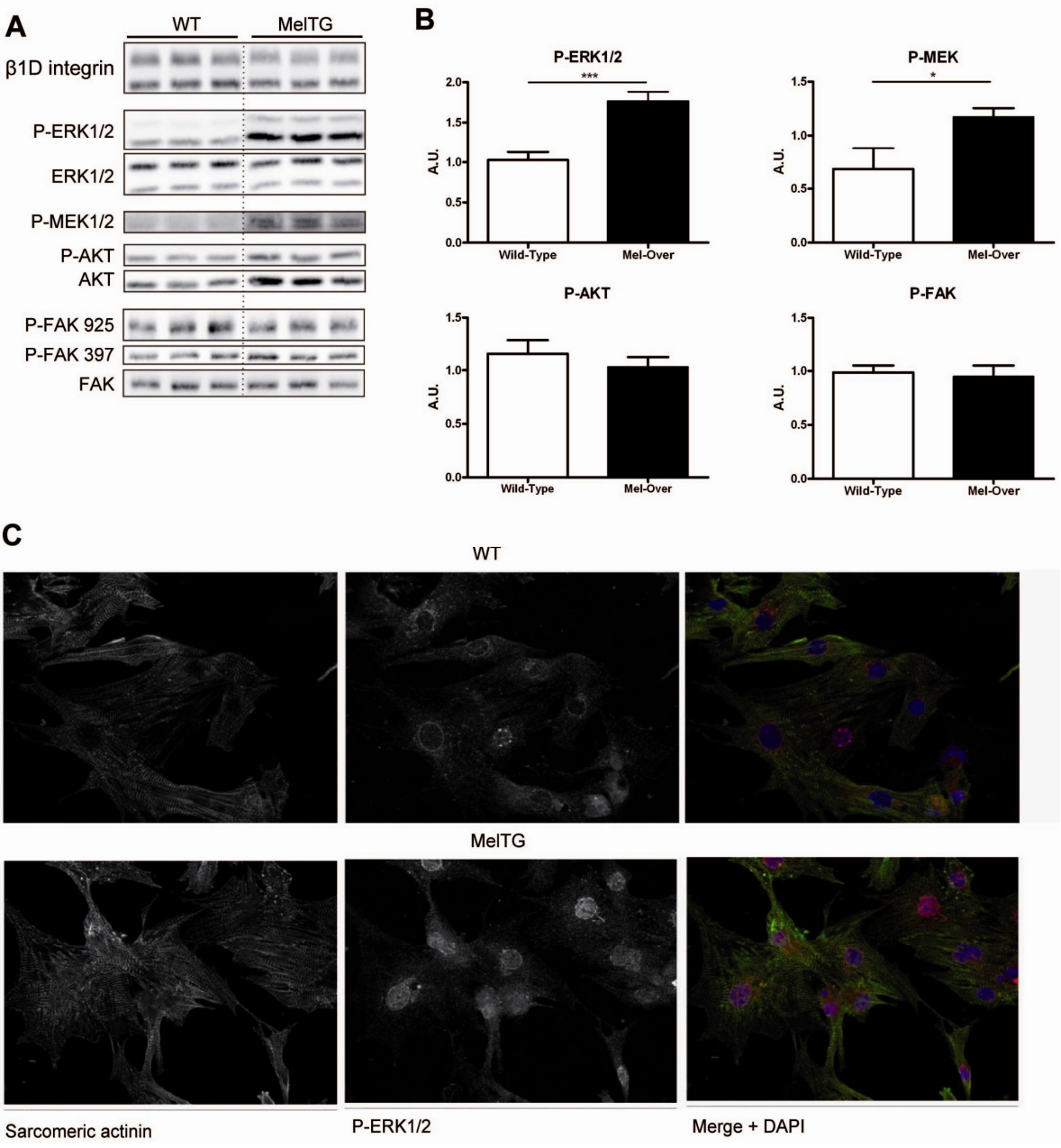
A
WT
MelTG
β1D integrin
P-ERK1/2
ERK1/2
P-MEK1/2
P-AKT
AKT
P-FAK 925
P-FAK 397
FAK
B
P-ERK1/2
***
P-MEK
*
P-AKT
P-FAK
A.U.
Wild-Type
Mel-Over
C
WT
MelTG
Sarcomeric actinin
P-ERK1/2
Merge + DAPI

**Figure 9**

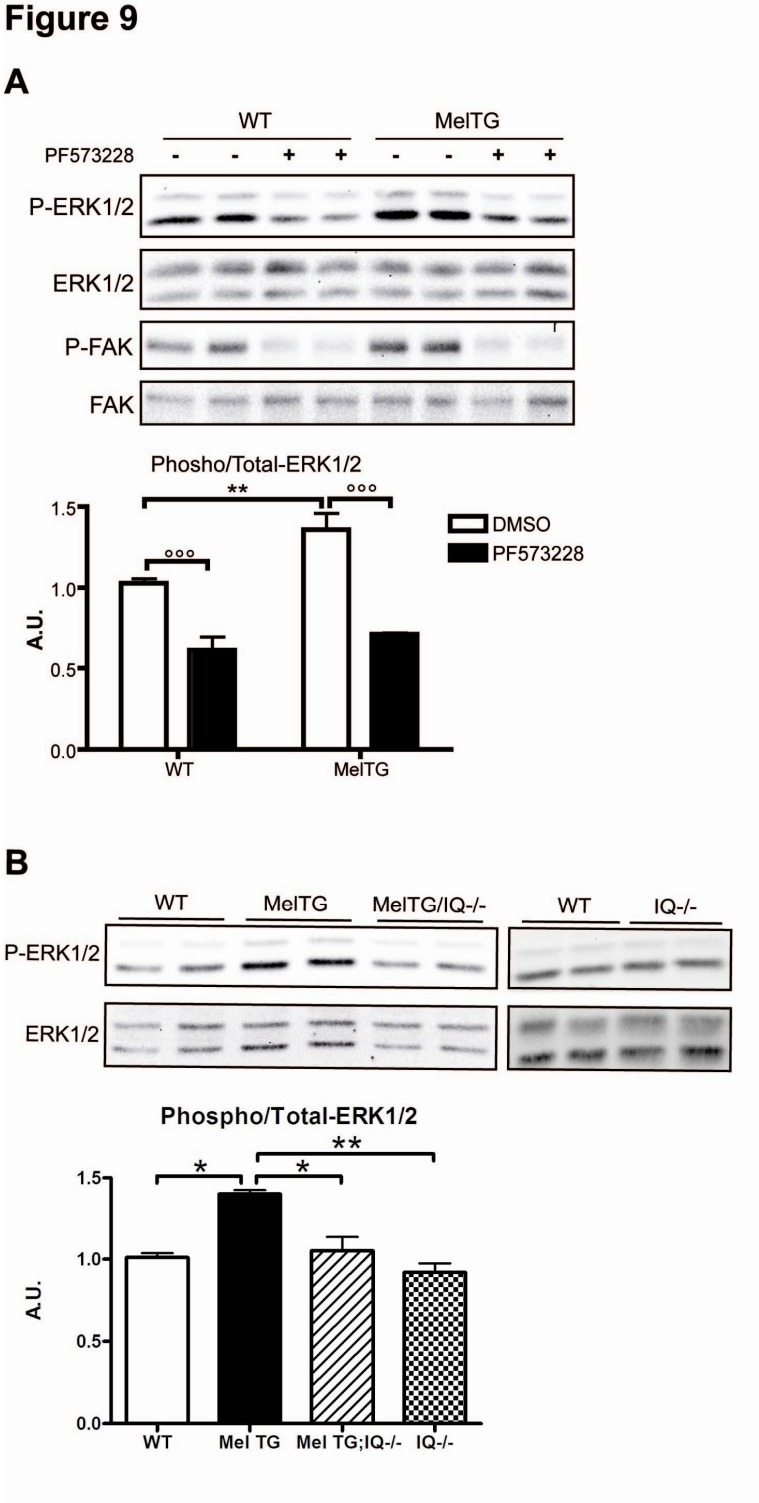
A
WT
MelTG
PF573228
- - + + - - + +
P-ERK1/2
ERK1/2
P-FAK
FAK
Phosho/Total-ERK1/2
**
°°°
°°°
1.5
1.0
0.5
0.0
A.U.
DMSO
PF573228
WT
MelTG
B
WT
MelTG
MelTG/IQ-/-
WT
IQ-/-
P-ERK1/2
ERK1/2
Phospho/Total-ERK1/2
**
*
*
1.5
1.0
0.5
0.0
A.U.
WT
Mel TG
Mel TG;IQ-/-
IQ-/-

**Figure 10**

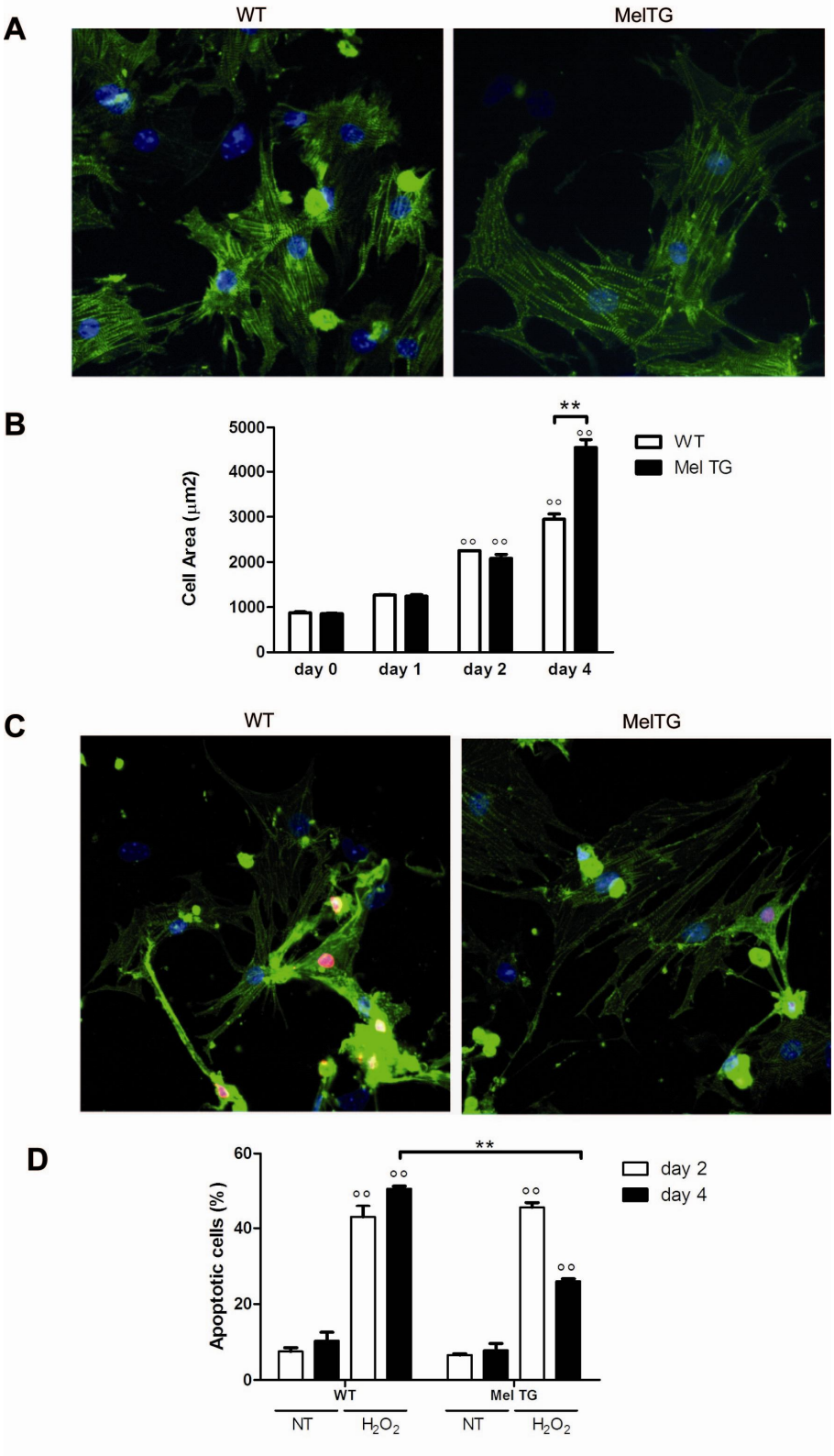
A
WT
MelTG
B
Cell Area (µm2)
5000
4000
3000
2000
1000
0
day 0
day 1
day 2
day 4
**
°°
WT
Mel TG
C
WT
MelTG
D
Apoptotic cells (%)
60
40
20
0
**
°°
day 2
day 4
WT
Mel TG
NT
H2O2
NT
H2O2

**Figure 11**

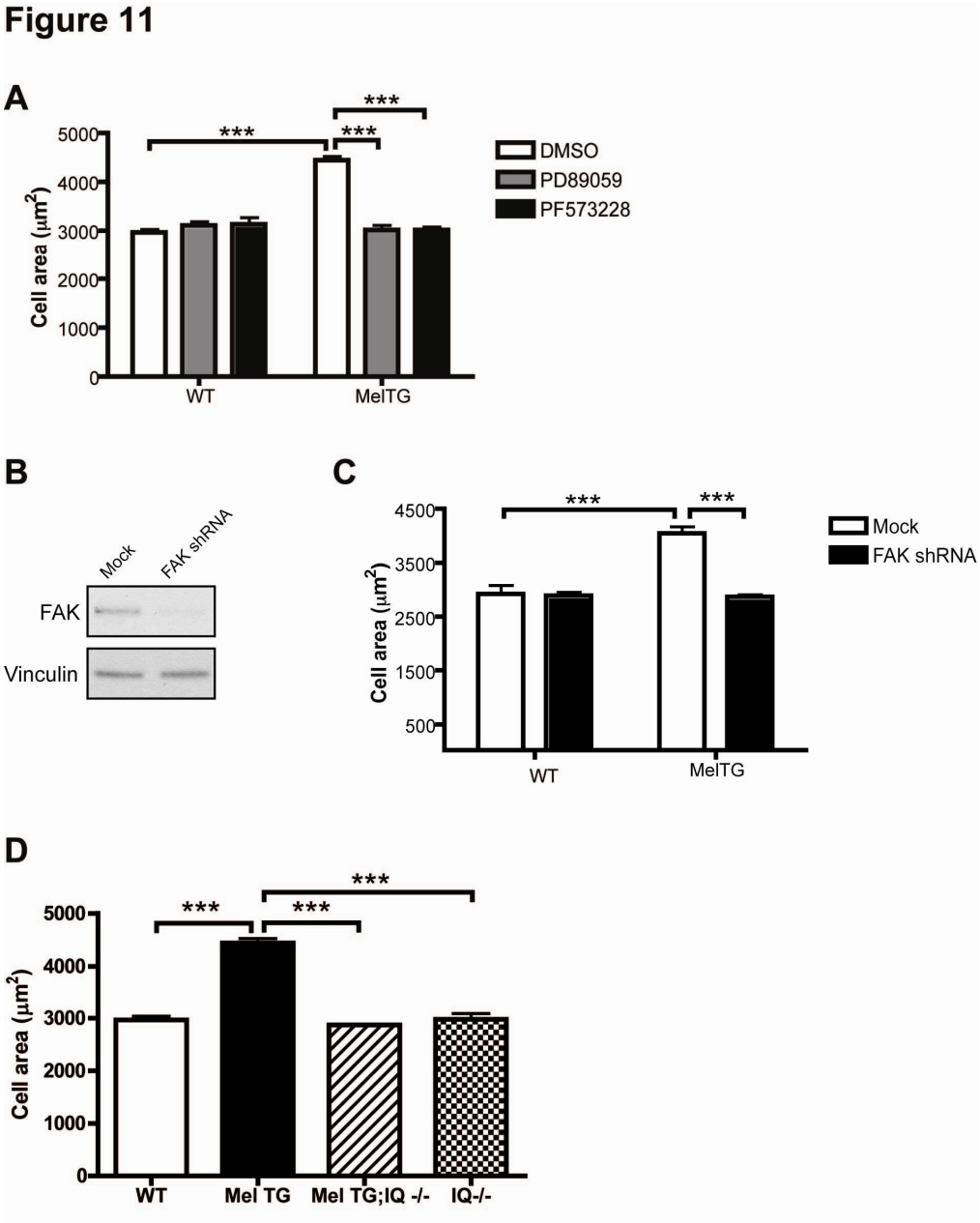
A
***
***
***
5000
4000
3000
2000
1000
0
Cell area (μm²)
WT
MelTG
DMSO
PD89059
PF573228
B
Mock
FAK shRNA
FAK
Vinculin
C
***
***
4500
3500
2500
1500
500
Cell area (μm²)
WT
MelTG
Mock
FAK shRNA
D
***
***
***
5000
4000
3000
2000
1000
0
Cell area (μm²)
WT
Mel TG
Mel TG;IQ -/-
IQ-/-

**Figure 12**

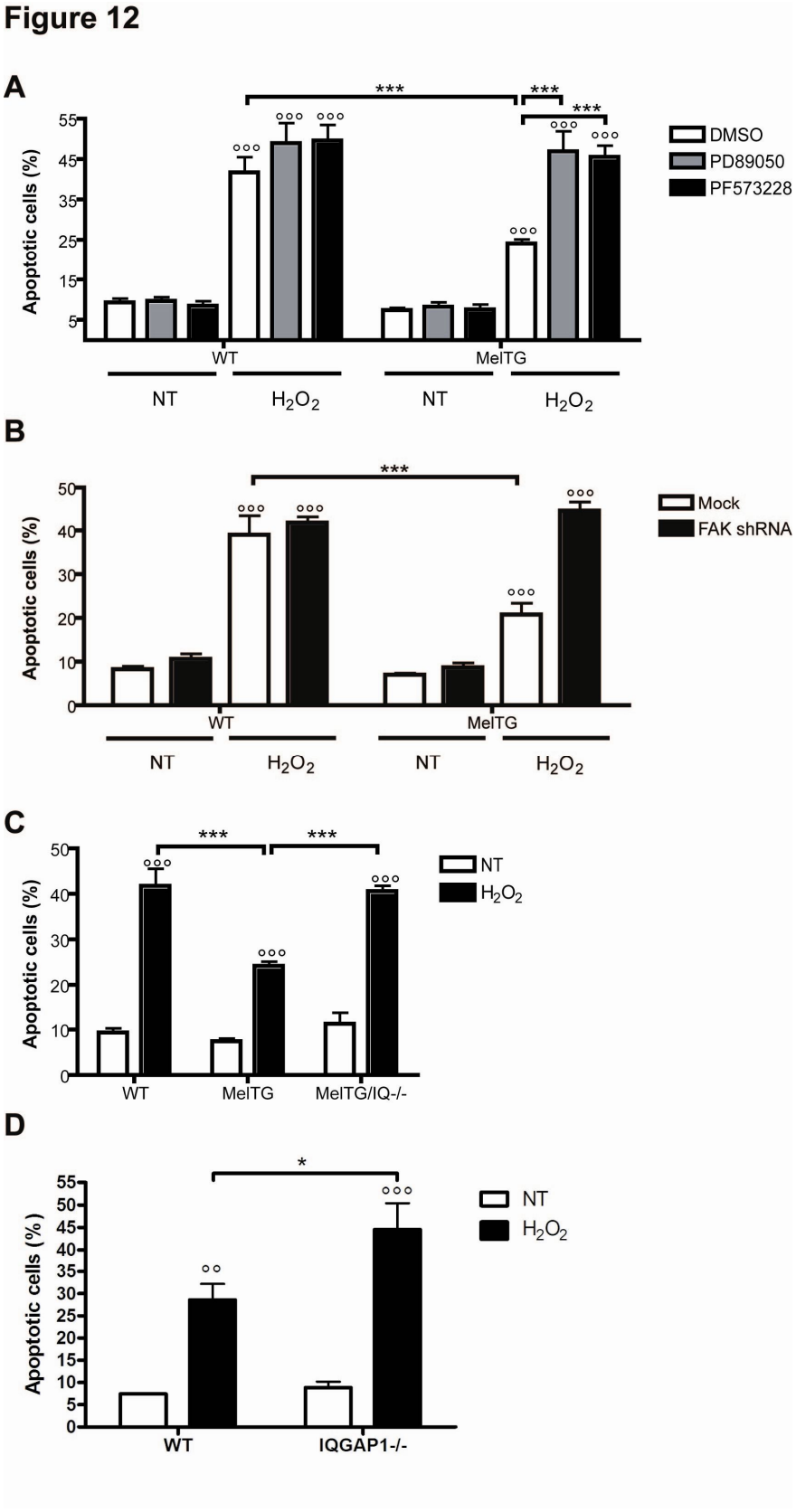
A
Apoptotic cells (%)
55
45
35
25
15
5
***
***
***
DMSO
PD89050
PF573228
WT
MelTG
NT
H2O2
NT
H2O2
B
Apoptotic cells (%)
50
40
30
20
10
0
***
Mock
FAK shRNA
WT
MelTG
NT
H2O2
NT
H2O2
C
Apoptotic cells (%)
50
40
30
20
10
0
***
***
NT
H2O2
WT
MelTG
MelTG/IQ-/-
D
Apoptotic cells (%)
55
50
45
40
35
30
25
20
15
10
5
0
*
NT
H2O2
WT
IQGAP1-/-

**FIGURE LEGENDS.**

**Figure 1. Melusin_bound MAPKs are activated by aortic banding (AB)**

(B) Immunoprecipitation of Melusin from sham-operated or subjected to 10 minutes AB Melusin-overexpressing (MelTG) hearts. Melusin-null hearts were used as negative controls. Co-immunoprecipitated proteins were visualized by Western blot analysis. Input: heart total protein extract loaded on the same Western blot as reference for molecular weights. Quantification of the co-precipitated proteins is shown in the graph (n=10/group). (C) ERK1/2 kinase assays were performed using GST-ELK1 as a substrate on Melusin immunocomplexes obtained from sham-operated or subjected to 10 min AB MelTG hearts. ERK1/2 kinase activity has been revealed by Western blot analysis with anti-phospho ELK1 (Ser 338) (n=6/group). (D) ERK1/2 kinase assay performed on Melusin immunocomplex in absence or presence of 1µM MEK1/2 inhibitor PD89059 (n=3/group). *$p<0.05$; ***$p<0.001$.

**Figure 2. Melusin interacts with FAK and the MAPK scaffold IQGAP1.**

(A) Western blot analysis of tyrosine phosphorylated proteins on Melusin immunocomplexes from MelTG hearts. (B) FAK co-immunoprecipitation revealed by Western blot on Melusin immunocomplexes isolated from sham and 10 minutes banded MelTG hearts (n=4 mice/group). Melusin-null hearts were used as negative controls. (C) Coomassie blue staining of Melusin immunoprecipitation from MelTG hearts. Indicated bands have been cut out to be subjected to mass spectrometry analysis. (D) IQGAP1, KSR-1 and paxillin Western blot on Melusin immunocomplexes isolated from sham and 10 minutes banded MelTG hearts (n=4

mice/group). Melusin null hearts have been used as negative controls. Input: heart total protein extract.

**Fig. 3. Melusin-bound ERK1/2 activation requires FAK and IQGAP1**

(A) ERK1/2 kinase assays performed on Melusin immunocomplexes obtained from sham-operated or subjected to 10 min AB MelTG hearts, in the absence or presence of 0.1 μM FAK inhibitor PF537228. ERK1/2 kinase activity was revealed by Western blot analysis with anti-phospho ELK1 (Ser 338) (n=4/group). (B) FAK kinase assays performed on Melusin immunocomplex obtained from sham-operated or subjected to 10 min AB MelTG hearts. FAK kinase activity was assayed using GST-$FAK_{378-406}$ as a substrate, and revealed by Western blot analysis with anti phospho-FAK (Tyr 397) (n=3/group). Melusin-null hearts were used as negative controls. (C) FAK kinase activity measured on FAK immunocomplexes obtained from sham-operated or subjected to 10 min AB WT hearts. FAK kinase activity was revealed by Western blotting with anti-phospho-FAK (Tyr 397) (n=4/group). (D) ERK1/2 kinase assay performed on Melusin immunocomplex obtained from sham-operated or subjected to 10 min AB MelTG and MelTG/IQGAP1null hearts (MelTG/IQ-/-). ERK1/2 kinase activity was revealed by Western blot analysis with anti-phospho ELK1 (Ser 338) (n=4/group). Melusin null hearts were used as negative controls.

**Figure 4. Mapping of domains involved in Melusin-IQGAP1 interaction.**

(A) Scheme of the recombinant MBP-fused IQGAP1 fragments used in pull-down experiments. The abilitiy of IQGAP1 fragments to interact with Melusin is indicated

as evaluated by pull-down experiments (nt: not tested). (B) Representative pull-down assay to test the ability of IQGAP1 fragments to interact with melusin in heart protein extracts. MBP alone has been used as negative control (Western blot is representative of 4 independent experiments). Recombinant proteins used in the pull-down were visualized by Coomassie staining (lower panel). Input: heart total protein extract. (C) Pull-down assay to test the ability of recombinant MBP-fused full length Melusin, Melusin CS domain or Melusin CHORD domains to interact with IQGAP1 in wild type heart protein extracts (Western blot is representative of 4 independent experiments). MBP alone was used as negative control. Recombinant proteins used in the pull-down were visualized by Coomassie staining (lower panel). Input: heart total protein extract. (D-E) Representative pull-down assays performed using the indicated recombinant purified GST-fused melusin fragments and MBP-fused IQGAP1 fragments. The interactions were revealed using anti-GST antibodies (Western blots are representative of 3 independent experiments). Recombinant proteins used in the pull-down were visualized by Coomassie staining (lower panels).

**Figure 5. IQGAP1 interactions with C-Raf1, MEK1/2, ERK1/2 and Hsp90.**

(A) Scheme of the recombinant MBP-fused IQGAP1 fragments used in pull-down experiments. The abilitiy of IQGAP1 fragments to interact with the indicated proteins is indicated as evaluated by pull-down experiments (nt: not tested). (B) Representative pull-down assay to test the ability of IQGAP1 fragments to interact with C-Raf or B-Raf in heart protein extracts. MBP alone has been used as negative control (Western blot is representative of 4 independent experiments). Recombinant proteins used in the pull-down were visualized by Coomassie staining (lower panel).

Input: heart total protein extract. (C) Representative Western blot of a pull-down assay to test the ability of IQGAP1 fragments to interact with c-Raf, MEK1/2 and ERK1/2 in both wild type and Melusin-null hearts. MBP alone has been used as a negative control (Western blots are representative of 3 independent experiments). Recombinant proteins used in pull-down experiments were visualized by Coomassie staining (lower panel). Input: heart total protein extract. (D) Representative Western blot of an Hsp90 immunoprecipitation to test the co-immunoprecipitation of IQGAP1 both in wild-type and Melusin-null hearts. An unrelated rabbit polyclonal antibody against MBP (IgG) was used as a negative control (Western blots are representative of 5 independent experiments). Input: heart total protein extract.

**Figure 6. Mapping of domains involved in Melusin-FAK interaction.**

(A) Scheme of the recombinant MBP or GST-fused FAK fragments used in pull-down experiments. The abilitiy of FAK fragments to interact with Melusin is indicated as evaluated by pull-down experiments. (B-C) Representative pull-down assays to test the ability of FAK fragments to interact with Melusin in heart protein extracts. MBP alone has been used as negative control (Western blot are representative of 2 independent experiments). Recombinant proteins used in the pull-down were visualized by Coomassie staining (lower panel). Input: heart total protein extract.

**Figure 7. Development of an *in vitro* model of mouse neonatal cardiomyocytes.**

(A) Western blot with the indicated antibodies of total protein extract from cultures of cardiac fibroblast (CF) and cardiac myocytes (CM) extracted from neonatal mice.

(B) Immunofluorescence of cultures of CM. Cells were stained with an antibody against sarcomeric alpha-actinin (green), phalloidin (red), and DAPI (blue). A merged image of the three stainings is reported in pseudocolors. (C) Western blot of CM extracted from wild-type (WT) and Melusin-overexpressing (MelTG) mice.

**Figure 8. Analysis of signalling pathways activation in MelTG NMC.**

(A-B) Western blot with antibodies developed against the total of phosporilated form of the indicated signalling proteins. NMC extracted from MelTG hearts were compared with WT counterparts. B1D integrin was used as a loading control. The graphs show the densitometric quantifications of the Western blot bands (n=7/group). Data are expressed in arbitrary units (A.U.) as the ratio of the phosporilation and total form of each signalling molecule. *p<0.05; ***p<0.001. (C) Immunofluorescence of NMC from WT or MelTG mice. Cells were stained with antibodies against sarcomeric alpha-actinin (green) and phospo-ERK1/2 (red). Nuclei were counterstained with DAPI (blue). Black and white images are reported on the left and in the center for sarcomeric actinin and phospho-ERK1/2 respectively, while merged images of the three stainings are in pseudocolors on the right.

**Figure 9. Analysis of the role of FAK and IQGAP1 in Melusin-dependent ERK1/2 activation.**

(A) Representative Western blot of the phosphorylation and total protein levels of ERK1/2 and FAK on WT and MelTG NMC untreated or treated with 3 μM PF537228. Densitometric quantification of Western blot bands is shown in the graph (n=4/group). **p<0.01 vs WT; °°°p<0.001 vs DMSO. (B) Western blot analysis of

phospho and total-ERK1/2 on NMC obtained from WT, MelTG, MelTG/IQGAP1null (MelTg/IQ-/-), and IQGAP1 null (IQ-/-) mice. The graph shows the densitometric quantification of Western blot bands (n=4/group). *p<0.5; **p<0.01.

**Figure 10. Cellular phenotypes triggered by Melusin overexpression in NMC.**

(A) Representative images of day 4 WT and MelTG NMC as analyzed by immunofluorescence after staining with the antibody against sarcomeric alpha-actinin (green) and DAPI (blue). (B) Measurements of cell area of WT and MelTG NMC at different time points of culture (n=4 cultures/group). °°p<0,01 vs day1;**p<0,01 vs WT. (C) Representative images of day 4 WT and MelTG NMC after H2O2 treatment. Apoptosis was evidenced by TUNEL reaction, and cells were further stained with the antibody against sarcomeric alpha-actinin (green) and DAPI (blue). (D) Quantification of the percentage of apoptotic WT and MelTG NMC at day 2 and 4 of cultures. Non treated (NT) cells were compared with H202 treated ones (n=4 cultures/group). °°p<0,01 ws NT; **p<0,01 vs WT.

**Figure 11. Analysis of the role of FAK and IQGAP1 in Melusin-dependent NMC hypertrophy.**

(A) Measures of cell area of WT and MelTG NMC at day 4 of culture, either untreated (DMSO) or treated with PD89059 or PF573228 for 48 hours. (n=5 cultures/group). ***p<0,001. (B) Representative Western blots for FAK protein levels performed on cardiomyocytes infected with lentiviral particles encoding for FAK shRNA or control viruses (Mock). Vinculin has been used as a control for

loading and RNA interference specificity. (C) Cardiomyocytes surface area measured on infected (GFP positive) WT and MelTG cells (n=4 cultures/group). (D) Measuements of cell area of WT, MelTG, MelTG/IQ-/- and IQ-/- NMC (5 cultures/group).

**Figure 12. Analysis of the role of FAK and IQGAP1 in Melusin-dependent NMC apoptosis.**

(A) Percentage of apoptotic cardiomyocytes after H2O2 treatment, as indicated by TUNEL nuclear staining. WT and MelTG cells were either untreated (DMSO) or treated with PD89059 or PF573228 for 18h after oxidative challenge. (5 cultures/group). °°°p<0,001 vs NT; ***p<0,001 (B) Apoptotic cells after H2O2 treatment in WT and MelTG cells that were previously infected with either shRNA-carrying or control (Mock) lentiviral vectors. (3 cultures/group). °°°p<0,001 vs NT; ***p<0,001. (C-D) Percentage of apoptotic cardiomyocytes after H2O2 challenge in WT, MelTG, MelTG/IQ-/- and IQ-/- cultures (5 cultures/group). °°p<0,01 vs NT; °°°p<0,001 vs NT; *p<0,5; ***p<0,001.

## BIBLIOGRAHPY


1. Awasthi, A., A. Samarakoon, H. Chu, R. Kamalakannan, L. A. Quilliam, M. Chrzanowska-Wodnicka, G. C. White, 2nd, and S. Malarkannan. Rap1b facilitates NK cell functions via IQGAP1-mediated signalosomes. J Exp Med 207:1923-38.
2. Balzac, F., A. M. Belkin, V. E. Koteliansky, Y. V. Balabanov, F. Altruda, L. Silengo, and G. Tarone. 1993. Expression and functional analysis of a cytoplasmic domain variant of the beta 1 integrin subunit. J Cell Biol 121:171-8.
3. Brancaccio, M., L. Fratta, A. Notte, E. Hirsch, R. Poulet, S. Guazzone, M. De Acetis, C. Vecchione, G. Marino, F. Altruda, L. Silengo, G. Tarone, and G. Lembo. 2003. Melusin, a muscle-specific integrin beta1-interacting protein, is required to prevent cardiac failure in response to chronic pressure overload. Nat Med 9:68-75.
4. Brancaccio, M., S. Guazzone, N. Menini, E. Sibona, E. Hirsch, M. De Andrea, M. Rocchi, F. Altruda, G. Tarone, and L. Silengo. 1999. Melusin is a new muscle-specific interactor for beta(1) integrin cytoplasmic domain. J Biol Chem 274:29282-8.
5. Braunwald, E., and M. R. Bristow. 2000. Congestive heart failure: fifty years of progress. Circulation 102:IV14-23.
6. Briggs, M. W., and D. B. Sacks. 2003. IQGAP proteins are integral components of cytoskeletal regulation. EMBO Rep 4:571-4.
7. Brown, M. D., and D. B. Sacks. 2006. IQGAP1 in cellular signaling: bridging the GAP. Trends Cell Biol 16:242-9.
8. Bueno, O. F., L. J. De Windt, K. M. Tymitz, S. A. Witt, T. R. Kimball, R. Klevitsky, T. E. Hewett, S. P. Jones, D. J. Lefer, C. F. Peng, R. N. Kitsis, and J. D. Molkentin. 2000. The MEK1-ERK1/2 signaling pathway promotes compensated cardiac hypertrophy in transgenic mice. Embo J 19:6341-50.
9. Burch, G. E., C. T. Ray, and J. A. Cronvich. 1952. Certain mechanical peculiarities of the human cardiac pump in normal and diseased states. Circulation 5:504-13.
10. Cai, X., D. Lietha, D. F. Ceccarelli, A. V. Karginov, Z. Rajfur, K. Jacobson, K. M. Hahn, M. J. Eck, and M. D. Schaller. 2008. Spatial and temporal regulation of focal adhesion kinase activity in living cells. Mol Cell Biol 28:201-14.
11. Casar, B., I. Arozarena, V. Sanz-Moreno, A. Pinto, L. Agudo-Ibanez, R. Marais, R. E. Lewis, M. T. Berciano, and P. Crespo. 2009. Ras subcellular localization defines

extracellular signal-regulated kinase 1 and 2 substrate specificity through distinct utilization of scaffold proteins. Mol Cell Biol 29:1338-53.

12. Chen, Q., T. H. Lin, C. J. Der, and R. L. Juliano. 1996. Integrin-mediated activation of MEK and mitogen-activated protein kinase is independent of Ras [corrected]. J Biol Chem 271:18122-7.
13. Cooper, L. A., T. L. Shen, and J. L. Guan. 2003. Regulation of focal adhesion kinase by its amino-terminal domain through an autoinhibitory interaction. Mol Cell Biol 23:8030-41.
14. De Acetis, M., A. Notte, F. Accornero, G. Selvetella, M. Brancaccio, C. Vecchione, M. Sbroggio, F. Collino, B. Pacchioni, G. Lanfranchi, A. Aretini, R. Ferretti, A. Maffei, F. Altruda, L. Silengo, G. Tarone, and G. Lembo. 2005. Cardiac overexpression of melusin protects from dilated cardiomyopathy due to long-standing pressure overload. Circ Res 96:1087-94.
15. DiMichele, L. A., J. T. Doherty, M. Rojas, H. E. Beggs, L. F. Reichardt, C. P. Mack, and J. M. Taylor. 2006. Myocyte-restricted focal adhesion kinase deletion attenuates pressure overload-induced hypertrophy. Circ Res 99:636-45.
16. Dorn, G. W., 2nd, J. Robbins, and P. H. Sugden. 2003. Phenotyping hypertrophy: eschew obfuscation. Circ Res 92:1171-5.
17. Favata, M. F., K. Y. Horiuchi, E. J. Manos, A. J. Daulerio, D. A. Stradley, W. S. Feeser, D. E. Van Dyk, W. J. Pitts, R. A. Earl, F. Hobbs, R. A. Copeland, R. L. Magolda, P. A. Scherle, and J. M. Trzaskos. 1998. Identification of a novel inhibitor of mitogen-activated protein kinase kinase. J Biol Chem 273:18623-32.
18. Frame, M. C., H. Patel, B. Serrels, D. Lietha, and M. J. Eck. The FERM domain: organizing the structure and function of FAK. Nat Rev Mol Cell Biol 11:802-14.
19. Franchini, K. G., C. F. Clemente, and T. M. Marin. 2009. Focal adhesion kinase signaling in cardiac hypertrophy and failure. Braz J Med Biol Res 42:44-52.
20. Fukuyo, Y., C. R. Hunt, and N. Horikoshi. Geldanamycin and its anti-cancer activities. Cancer Lett 290:24-35.
21. Guo, W., and F. G. Giancotti. 2004. Integrin signalling during tumour progression. Nat Rev Mol Cell Biol 5:816-26.
22. Harris, I. S., S. Zhang, I. Treskov, A. Kovacs, C. Weinheimer, and A. J. Muslin. 2004. Raf-1 kinase is required for cardiac hypertrophy and cardiomyocyte survival in response to pressure overload. Circulation 110:718-23.

23. Heil, A., A. R. Nazmi, M. Koltzscher, M. Poeter, J. Austermann, N. Assard, J. Baudier, K. Kaibuchi, and V. Gerke. S100P is a novel interaction partner and regulator of IQGAP1. J Biol Chem 286:7227-38.
24. Heineke, J., and J. D. Molkentin. 2006. Regulation of cardiac hypertrophy by intracellular signalling pathways. Nat Rev Mol Cell Biol 7:589-600.
25. Hill, J. A., and E. N. Olson. 2008. Cardiac plasticity. N Engl J Med 358:1370-80.
26. Hood, J. D., R. Frausto, W. B. Kiosses, M. A. Schwartz, and D. A. Cheresh. 2003. Differential alphav integrin-mediated Ras-ERK signaling during two pathways of angiogenesis. J Cell Biol 162:933-43.
27. Hunter, J. J., N. Tanaka, H. A. Rockman, J. Ross, Jr., and K. R. Chien. 1995. Ventricular expression of a MLC-2v-ras fusion gene induces cardiac hypertrophy and selective diastolic dysfunction in transgenic mice. J Biol Chem 270:23173-8.
28. Hynes, R. O. 2002. Integrins: bidirectional, allosteric signaling machines. Cell 110:673-87.
29. Jessup, M., and S. Brozena. 2003. Heart failure. N Engl J Med 348:2007-18.
30. Kehat, I., and J. D. Molkentin. Extracellular signal-regulated kinase 1/2 (ERK1/2) signaling in cardiac hypertrophy. Ann N Y Acad Sci 1188:96-102.
31. Kolch, W. 2005. Coordinating ERK/MAPK signalling through scaffolds and inhibitors. Nat Rev Mol Cell Biol 6:827-37.
32. Kolch, W. 2000. Meaningful relationships: the regulation of the Ras/Raf/MEK/ERK pathway by protein interactions. Biochem J 351 Pt 2:289-305.
33. Krumholz, H. M., M. Larson, and D. Levy. 1995. Prognosis of left ventricular geometric patterns in the Framingham Heart Study. J Am Coll Cardiol 25:879-84.
34. Lal, H., S. K. Verma, M. Smith, R. S. Guleria, G. Lu, D. M. Foster, and D. E. Dostal. 2007. Stretch-induced MAP kinase activation in cardiac myocytes: differential regulation through beta1-integrin and focal adhesion kinase. J Mol Cell Cardiol 43:137-47.
35. Li, S., Q. Wang, A. Chakladar, R. T. Bronson, and A. Bernards. 2000. Gastric hyperplasia in mice lacking the putative Cdc42 effector IQGAP1. Mol Cell Biol 20:697-701.
36. Lietha, D., X. Cai, D. F. Ceccarelli, Y. Li, M. D. Schaller, and M. J. Eck. 2007. Structural basis for the autoinhibition of focal adhesion kinase. Cell 129:1177-87.
37. Lips, D. J., O. F. Bueno, B. J. Wilkins, N. H. Purcell, R. A. Kaiser, J. N. Lorenz, L. Voisin, M. K. Saba-El-Leil, S. Meloche, J. Pouyssegur, G. Pages, L. J. De Windt, P.

A. Doevendans, and J. D. Molkentin. 2004. MEK1-ERK2 signaling pathway protects myocardium from ischemic injury in vivo. Circulation 109:1938-41.

38. Lorenz, K., J. P. Schmitt, E. M. Schmitteckert, and M. J. Lohse. 2009. A new type of ERK1/2 autophosphorylation causes cardiac hypertrophy. Nat Med 15:75-83.
39. Manyari, D. E. 1990. Prognostic implications of echocardiographically determined left ventricular mass in the Framingham Heart Study. N Engl J Med 323:1706-7.
40. McNulty, D. E., Z. Li, C. D. White, D. B. Sacks, and R. S. Annan. Map kinase scaffold IQGAP1 binds the EGF receptor and modulates its activation. J Biol Chem.
41. Meyer, R. D., D. B. Sacks, and N. Rahimi. 2008. IQGAP1-dependent signaling pathway regulates endothelial cell proliferation and angiogenesis. PLoS One 3:e3848.
42. Mitra, S. K., D. A. Hanson, and D. D. Schlaepfer. 2005. Focal adhesion kinase: in command and control of cell motility. Nat Rev Mol Cell Biol 6:56-68.
43. Pham, C. G., A. E. Harpf, R. S. Keller, H. T. Vu, S. Y. Shai, J. C. Loftus, and R. S. Ross. 2000. Striated muscle-specific beta(1D)-integrin and FAK are involved in cardiac myocyte hypertrophic response pathway. Am J Physiol Heart Circ Physiol 279:H2916-26.
44. Pratt, W. B., and D. O. Toft. 2003. Regulation of signaling protein function and trafficking by the hsp90/hsp70-based chaperone machinery. Exp Biol Med (Maywood) 228:111-33.
45. Purcell, N. H., B. J. Wilkins, A. York, M. K. Saba-El-Leil, S. Meloche, J. Robbins, and J. D. Molkentin. 2007. Genetic inhibition of cardiac ERK1/2 promotes stress-induced apoptosis and heart failure but has no effect on hypertrophy in vivo. Proc Natl Acad Sci U S A 104:14074-9.
46. Ramos, J. W. 2008. The regulation of extracellular signal-regulated kinase (ERK) in mammalian cells. Int J Biochem Cell Biol 40:2707-19.
47. Ren, J. G., Z. Li, D. L. Crimmins, and D. B. Sacks. 2005. Self-association of IQGAP1: characterization and functional sequelae. J Biol Chem 280:34548-57.
48. Ren, J. G., Z. Li, and D. B. Sacks. 2008. IQGAP1 integrates Ca2+/calmodulin and B-Raf signaling. J Biol Chem 283:22972-82.
49. Ren, J. G., Z. Li, and D. B. Sacks. 2007. IQGAP1 modulates activation of B-Raf. Proc Natl Acad Sci U S A 104:10465-9.
50. Roy, M., Z. Li, and D. B. Sacks. 2004. IQGAP1 binds ERK2 and modulates its activity. J Biol Chem 279:17329-37.

51. Roy, M., Z. Li, and D. B. Sacks. 2005. IQGAP1 is a scaffold for mitogen-activated protein kinase signaling. Mol Cell Biol 25:7940-52.
52. Sacks, D. B. 2006. The role of scaffold proteins in MEK/ERK signalling. Biochem Soc Trans 34:833-6.
53. Santos, S. D., P. J. Verveer, and P. I. Bastiaens. 2007. Growth factor-induced MAPK network topology shapes Erk response determining PC-12 cell fate. Nat Cell Biol 9:324-30.
54. Sbroggio, M., D. Carnevale, A. Bertero, G. Cifelli, E. De Blasio, G. Mascio, E. Hirsch, W. F. Bahou, E. Turco, L. Silengo, M. Brancaccio, G. Lembo, and G. Tarone. IQGAP1 regulates ERK1/2 and AKT signaling in the heart and sustains functional remodeling upon pressure overload. Cardiovasc Res.
55. Sbroggio, M., R. Ferretti, E. Percivalle, M. Gutkowska, A. Zylicz, W. Michowski, J. Kuznicki, F. Accornero, B. Pacchioni, G. Lanfranchi, J. Hamm, E. Turco, L. Silengo, G. Tarone, and M. Brancaccio. 2008. The mammalian CHORD-containing protein melusin is a stress response protein interacting with Hsp90 and Sgt1. FEBS Lett 582:1788-94.
56. Schrick, C., A. Fischer, D. P. Srivastava, N. C. Tronson, P. Penzes, and J. Radulovic. 2007. N-cadherin regulates cytoskeletally associated IQGAP1/ERK signaling and memory formation. Neuron 55:786-98.
57. Schulte, T. W., W. G. An, and L. M. Neckers. 1997. Geldanamycin-induced destabilization of Raf-1 involves the proteasome. Biochem Biophys Res Commun 239:655-9.
58. Serrels, B., A. Serrels, V. G. Brunton, M. Holt, G. W. McLean, C. H. Gray, G. E. Jones, and M. C. Frame. 2007. Focal adhesion kinase controls actin assembly via a FERM-mediated interaction with the Arp2/3 complex. Nat Cell Biol 9:1046-56.
59. Slack-Davis, J. K., S. T. Eblen, M. Zecevic, S. A. Boerner, A. Tarcsafalvi, H. B. Diaz, M. S. Marshall, M. J. Weber, J. T. Parsons, and A. D. Catling. 2003. PAK1 phosphorylation of MEK1 regulates fibronectin-stimulated MAPK activation. J Cell Biol 162:281-91.
60. Slack-Davis, J. K., K. H. Martin, R. W. Tilghman, M. Iwanicki, E. J. Ung, C. Autry, M. J. Luzzio, B. Cooper, J. C. Kath, W. G. Roberts, and J. T. Parsons. 2007. Cellular characterization of a novel focal adhesion kinase inhibitor. J Biol Chem 282:14845-52.
61. Vadali, K., X. Cai, and M. D. Schaller. 2007. Focal adhesion kinase: an essential kinase in the regulation of cardiovascular functions. IUBMB Life 59:709-16.

62. Willis, M. S., and C. Patterson. Hold me tight: Role of the heat shock protein family of chaperones in cardiac disease. Circulation 122:1740-51.
63. Yablonski, D., I. Marbach, and A. Levitzki. 1996. Dimerization of Ste5, a mitogen-activated protein kinase cascade scaffold protein, is required for signal transduction. Proc Natl Acad Sci U S A 93:13864-9.
64. Yamaguchi, O., T. Watanabe, K. Nishida, K. Kashiwase, Y. Higuchi, T. Takeda, S. Hikoso, S. Hirotani, M. Asahi, M. Taniike, A. Nakai, I. Tsujimoto, Y. Matsumura, J. Miyazaki, K. R. Chien, A. Matsuzawa, C. Sadamitsu, H. Ichijo, M. Baccarini, M. Hori, and K. Otsu. 2004. Cardiac-specific disruption of the c-raf-1 gene induces cardiac dysfunction and apoptosis. J Clin Invest 114:937-43.
65. Yoon, S., and R. Seger. 2006. The extracellular signal-regulated kinase: multiple substrates regulate diverse cellular functions. Growth Factors 24:21-44.
66. Zhang, M., Y. Kadota, C. Prodromou, K. Shirasu, and L. H. Pearl. Structural basis for assembly of Hsp90-Sgt1-CHORD protein complexes: implications for chaperoning of NLR innate immunity receptors. Mol Cell 39:269-81.

**ACKNOWLEDGMENTS**

Thanks to Prof. Guido Tarone and Mara Brancaccio for giving me the opportunity to work in their research group, as well as for their precious advices in the developing of my thesis.

Thanks to Prof. Fiorella Altruda and Lorenzo Silengo for allowing me to work at the Molecular Biotechnology Center of the University of Turin.

Thanks to Prof. Emilia Turco for her help, advices and support.

Thanks to all the past and present members of Prof. Brancaccio and Tarone's laboratory for their invaluable advices, as well as their friendship in everyday work .

In particular, I would like to thank Dr. Mauro Sbroggiò, that supervised me from my first day of work, and taught me everything I know about doing research.

Thanks to Dr. Emanuele De Blasio that produced many of the expression constructs of IQGAP1 fragments, and that performed the first pull-down experiments.

Thanks to Dr. Federica Fusella, that produced the lentivirus and infected the cells for my experiments.

Thanks to Wadie F. Bahou and Brian Serrels for providing us respectively the IQGAP1-/- mice, and the FAK fragments-encoding expression vectors.

Last but not least, I would like to thank my mum and dad for all their help and support, especially during these long years of studies that they allowed me to pursue.

Finally, thanks to my girlfriend Caterina for her great support and patience. I love you.